

Spring 5-7-2010

# Investigation of the role of BAM9 in starch metabolism in *Arabidopsis thaliana*

Elizabeth Ann Steidle  
*James Madison University*

Follow this and additional works at: <https://commons.lib.jmu.edu/master201019>

 Part of the [Biology Commons](#)

---

## Recommended Citation

Steidle, Elizabeth Ann, "Investigation of the role of BAM9 in starch metabolism in *Arabidopsis thaliana*" (2010). *Masters Theses*. 384.  
<https://commons.lib.jmu.edu/master201019/384>

This Thesis is brought to you for free and open access by the The Graduate School at JMU Scholarly Commons. It has been accepted for inclusion in Masters Theses by an authorized administrator of JMU Scholarly Commons. For more information, please contact [dc\\_admin@jmu.edu](mailto:dc_admin@jmu.edu).

Investigation of the role of BAM9 in starch metabolism in *Arabidopsis thaliana*

Elizabeth Ann Steidle

A thesis submitted to the Graduate Faculty of

JAMES MADISON UNIVERSITY

In

Partial Fulfillment of the Requirements

for the degree of

Master of Arts or Science

Department of Biology

May 2010

## ACKNOWLEDGEMENTS

I would first like to thank my parents who have supported me in all of my endeavors and pushed me to achieve my Masters degree. I would like to thank Kevin Fedkenheuer, John Herlihy, John Marafino, and Lauren Saunders for all of their hard work in the lab and contributing to the results of my Thesis. I would also like to thank Sammy Mainiero and Matthew Lohr for making work in the lab so enjoyable. My time at JMU would not have been the same without you all.

For helping me get started with Real-Time PCR, I would like to thank Dr. Terrie Rife, Divya Bansal, and Dr. Elizabeth Doyle. My Real-Time efforts would not have meant a thing to me without your instruction. I want to give a special thanks to Dr. Elizabeth Doyle for not only helping me with Real-Time but also all of the other help she gave to me over the past two years. My Masters program would have been far more difficult without her.

Finally, I give the most thanks to Dr. Jonathan Monroe for being a great mentor! Without him my work would not have been possible. He taught me most of the molecular techniques I needed to complete this project and he was very patient during my incessant questioning. He is a great advisor, teacher, listener, and friend. He has opened my world to molecular biology and significantly influenced my career goals.

## TABLE OF CONTENTS

Acknowledgements.....	ii
Table of Contents.....	iii
List of Tables .....	iv
List of Figures .....	v
Abstract.....	vii
I. Introduction.....	1
$\beta$ -amylases and their role in starch metabolism.....	3
Does BAM9 have a role in starch metabolism?.....	8
II. Methods.....	13
Sequence Analysis and 3-D Modeling.....	13
Plant Material.....	13
Starch Quantification .....	13
Amylase Assays.....	16
Harvest and Homogenization.....	16
Amylase Assay.....	16
Protein Assay .....	17
Measuring RNA .....	17
Extraction of RNA .....	17
Reverse Transcription and Polymerase Chain Reaction.....	18
Protein Purification of BAM3 and BAM9.....	19
Generating a Recombinant Plasmid.....	19
Transformation of BL21 Cells and Protein Purification.....	23
Thin Layer Chromatography (TLC).....	24
III. Results.....	26
Phylogenetic Analysis of Arabidopsis $\beta$ -amylases.....	26
Sequence Analysis and 3-D Modeling.....	26
Starch Quantification .....	29
Amylase Assays.....	37
The Effect of BAM9 on the Expression of <i>BAM3</i> .....	37
Purification of BAM3 and BAM9 .....	40
Catalytic Activity of BAM9.....	45
IV. Discussion.....	50
V. Literature Cited.....	62

## LIST OF TABLES

Table 1. Accession Numbers and Gene names for $\beta$ -amylases used in this study...	14
Table 2. Primers used for semi-quantitative and Real-Time PCR.....	20
Table 3. Semi-quantitative PCR heating protocol.....	21
Table 4. Real-Time PCR protocol.....	22

## LIST OF FIGURES

Figure 1. Structure of Amylose (A). Structure of Amylopectin (B).....	2
Figure 2. Expression data for <i>BAM9</i> .....	11
Figure 3. A comparison of the expression data of <i>BAM9</i> and Disproportionating Enzyme1.....	12
Figure 4. Arabidopsis BAM proteins compared to poplar, grape, and rice BAM proteins.....	27
Figure 5. The amino acids of the $\beta$ -amylase active site comparing five active BAMs to the <i>BAM9</i> orthologs .....	30
Figure 6. A region of the amino acid sequence of the soybean $\beta$ -amylase aligned with five active Arabidopsis BAMs and five <i>BAM9</i> orthologs.....	31
Figure 7. Two views of a hypothetical 3D model of the <i>BAM9</i> protein generated using the threading program PHYRE .....	32
Figure 8. <i>bam9</i> T-DNA mutant does not show <i>BAM9</i> expression.....	34
Figure 9. Leaves stained with iodine for starch accumulation.....	35
Figure 10. Quantification of starch in <i>Arabidopsis thaliana</i> .....	36
Figure 11. Amylase activity in crude extracts from ~5 week old leaves of WT, <i>bam9</i> , <i>bam3</i> , and <i>bam3,9</i> mutants.....	38
Figure 12. Amylase activity in crude extracts from ~6 ½ week old leaves of WT, <i>bam9</i> , <i>bam3</i> , and <i>bam3,9</i> mutants.....	39
Figure 13. Semi-quantitative PCR comparing the expression of <i>BAM3</i> between the WT and the <i>bam9</i> mutant.....	41
Figure 14. Expression of the <i>bam3</i> gene in <i>bam9</i> mutant compared to the WT.....	42
Figure 15. An SDS-PAGE gel of <i>BAM9</i> purification.....	43
Figure 16. An SDS-PAGE gel of <i>BAM3</i> purification.....	44
Figure 17. Amylase activity of <i>BAM3</i> compared to the amylase activity of <i>BAM9</i> .....	47
Figure 18. Thin Layer Chromatography of oligosaccharide products after incubation with <i>BAM3</i> and <i>BAM9</i> (maltohexose and maltotriose).....	48

Figure 19. Thin Layer Chromoatography of oligosaccharide products after incubation with BAM3 and BAM (maltohexose and maltopentose).....	49
Figure 20. A working model for the role of BAM9 in starch metabolism.....	60
Figure 21. The effect of different knockout mutants on the working model of BAM9 function.....	61

## ABSTRACT

$\beta$ -amylases play an essential role in night time starch degradation in leaves. There are nine known  *$\beta$ -amylases (BAMs)* in *Arabidopsis thaliana*. This research is focused on BAM9, which is localized in the chloroplasts but is unique compared to active BAM proteins. First, alignments of BAM9 orthologs and catalytically active paralogs suggest that BAM9 may not be catalytically active and may not bind to starch, but it may bind to another molecule at a remote site. Secondly, microarray data shows a peak of *BAM9* expression at the dark/light transition which is contradictory to what one would expect for an active BAM protein. We propose that BAM9 is not directly involved in starch degradation. Starch quantification results show a starch accumulation phenotype in a *bam9* knockout mutant compared to the wild type (WT), implying that BAM9 is functional in starch metabolism. Amylase assays using pure BAM9 protein expressed in *E. coli* confirmed that BAM9 is catalytically inactive with starch, maltotriose, maltopentose, and maltohexose as the substrates. However, assays of crude leaf extracts from *bam9* knockout mutants reveal greater amylase activity than WT, suggesting that BAM9 may play a regulatory role at the transcriptional or the post-transcriptional level. The transcriptional regulation hypothesis was rejected after observing that the expression of BAM3 in the *bam9* mutant background was not different than WT. BAM1 and -3 are known to be phosphorylated and there is a chloroplast kinase that causes a starch accumulation phenotype when knocked out. We hypothesize that BAM9 acts upstream of this kinase, which may inactivate both BAM3 during the day and BAM1 during the night.



## INTRODUCTION

Starch is a storage molecule found in various organs of plants such as leaves, flowers, developing seeds, and root caps (Zeeman et al., 2002). It plays a major role in human and animal nutrition, and is used industrially. It is localized in plastids of plants (Lao et al., 1999) and during the day starch accumulates while at night starch is metabolized into sugar for energy (Sparla et al., 2006). The granular structure of starch is made of semicrystalline particles. Within the semicrystalline particles are double helices of glucose polymers which are amylose and amylopectin (Figure 1). Amylopectin is thought to make up 90% of the starch in leaves and is a polymer of  $\alpha$ -1, 4 linkages with occasional  $\alpha$ -1, 6 branches (Lloyd et al., 2005), while amylose molecules are not branched and only have  $\alpha$ -1, 4 glycosidic linkages (Figure 1). Arabidopsis starchless mutants have stunted growth when grown under a light/dark cycle (Casper et al., 1985) suggesting that the starch metabolism and synthesis cycle in plants is important.

There are many enzymes in plants that degrade starch including  $\alpha$ -amylase, limit dextrinase (debranching enzyme),  $\alpha$ -glucosidase and  $\beta$ -amylase (Zeeman et al., 2007).  $\alpha$ -amylases (AMY) are known to cleave amylose and amylopectin at  $\alpha$ -1, 4 glucosyl linkages. There are three AMYs found in Arabidopsis (Stanely et al., 2002). AMY3 is localized in the chloroplasts (Zeeman et al., 1998; Yu et al., 2005); however *amy3* knockout mutants do not show any starch accumulation phenotype (Yu et al., 2005). It is therefore believed that  $\alpha$ -amylases only play a minor role in starch metabolism (Stanely et al., 2002).

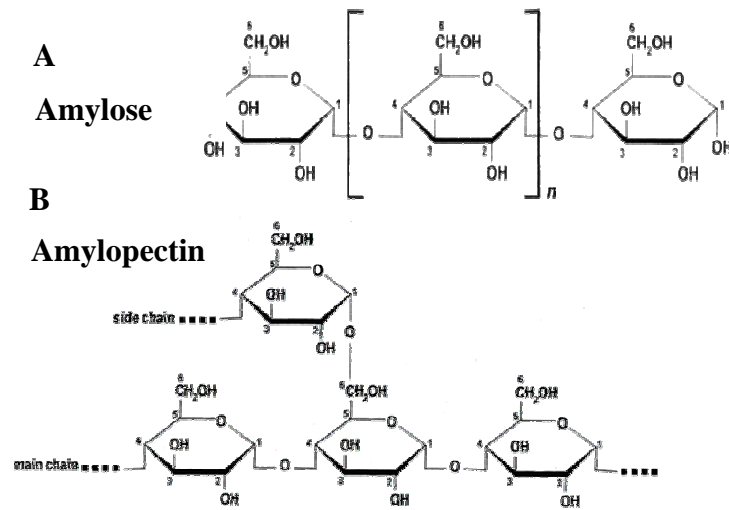


**Figure 1.** Structure of Amylose (A). Structure of Amylopectin (B). (Laurila and Bohlén, 2007)

Starch phosphorylation is important in starch degradation. In *Arabidopsis*, 1 in 2000 glucose residues in leaf starch carry phosphate groups at night (Yu et al., 2001). Starch granules are phosphorylated during starch degradation by glucan, water dikinase (GWD) at the C-6 position of glucosyl residues (Ritte et al., 2000, 2006). As well, the C-3 position of the glucosyl residues are phosphorylated by a different kinase, phosphoglucan, water dikinase (Baunsgaard et al., 2005; Knötting et al., 2005; Ritte et al., 2006). GWD has been reported to be more active during starch break down, in which  $\beta$ -amylases play the primary role. Edner et al. (2007) discovered that  $\beta$ -amylase activity is significantly increased if  $\beta$ -amylases work together with GWD *in vitro*. The phosphorylation is thought to disrupt the granular surface and allow  $\beta$ -amylases and isoamylases access to starch (Knötting et al., 2009; Edner et al., 2007). The debranching enzymes such as limit dextrinase and isoamylase begin to break down starch after  $\beta$ -amylases, cleaving the  $\alpha$ -1, 6 amylopectin linkages (Delatte et al., 2006). They break the branched glucans into linear glucans (Delatte et al., 2006).

#### *$\beta$ -amylases and their role in starch metabolism*

$\beta$ -amylases are the major contributor to starch breakdown in leaves (Fulton et al., 2008; Lao et al., 1999).  $\beta$ -amylases are exoamylases which break glycosidic bonds at  $\alpha$ -1, 4 glycosidic linkages of starch (Kaplan and Guy, 2004). They remove  $\beta$ -maltose, a disaccharide made up of two glucose molecules, from the non-reducing ends of starch (Sparla et al., 2006).

Plant species with reduced chloroplastic  $\beta$ -amylase activity degraded significantly less starch at night as compared with the wild-type plants (Scheidlig et al., 2002). Once

the maltose is cleaved from the starch molecule it is transported to the cytosol (Sparla et al., 2006). This is known because maltose levels increase in the leaves while starch is being broken down (Niittylä et al., 2004; Weise et al., 2004) and the chloroplast envelope is permeable to maltose (Weise et al., 2004). *mex1* knockout plants have been shown to accumulate maltose and starch in chloroplasts which led Niittylä et al. (2004) to conclude that maltose is transported to the cytosol via the maltose transporter, MEX1 (Niittylä et al., 2004; Weise et al., 2004).

The nucleotide and amino acid sequences of the  $\beta$ -amylases have helped researchers make hypotheses on their role in starch metabolism. There are nine genes coding for the  $\beta$ -amylases in *Arabidopsis*. Fulton et al. (2008) compared these *Arabidopsis* genes to those in two other species, rice (*Oryza sativa*) and poplar (*Populus sp*) in a phylogenetic analysis. The BAM genes fell into four subfamilies within the tree. *Arabidopsis* genes and their orthologs in poplar and rice were present in every subfamily (Fulton et al., 2008). The subfamilies consisted of subfamily I with BAM5 and -6, subfamily II with BAM1 and -3, subfamily III with BAM4 and -9 and subfamily IV with BAM7, -8, and -2 (the numbering system following the *Arabidopsis* BAMs). Some of the subfamilies include genes that are localized to the same organelle such as BAM1 and -3 which code for active chloroplastic enzymes (Lao et al., 1999; Sparla et al., 2006) and BAM7 and -8 which code for proteins that are localized to the nucleus (Zeeman, personal communication; Monroe, unpublished). But within subfamily IV not every protein has been found in the same localization. BAM2 is found in this subfamily with BAM7 and -8 but BAM2 is missing the N-terminal extension which contains a nuclear localization signal. Due to this, it is predicted that BAM2 underwent a deletion in the gene and that

could be the reason the role of BAM2 in starch metabolism seems to be minimal (Fulton et al., 2008).

The soybean  $\beta$ -amylase5 was crystallized, revealing that the  $\beta$ -amylase has three folding domains; the first is an N-terminal  $\alpha$ ,  $\beta$  barrel motif, the second is just an extension of the first and the third domain is the C-terminus with two parallel  $\beta$ -sheets (Mikami et al., 1993). Modeling studies resulted in identification of the amino acids within the active site (Mikami et al., 1993). It was discovered when observing a model of the soybean  $\beta$ -amylase that the product, maltose, binds to a deep pocket in the center of the molecule (Mikami et al., 1993). Fifteen amino acids were found to hydrogen bond to the first four glucosyl residues of the non-reducing end of starch (Mikami et al., 1993). Along the outside of the cavity of the active site in the soybean  $\beta$ -amylase a flexible loop was found (Totsuka and Fukazawa, 1996). These loops help  $\beta$ -amylases hold starch while releasing maltose during degradation (Kang et al. 2004). The flexible loop is thought to bind to the starch molecule during catalysis and then open to allow maltose out of the active site (Totsuka and Fukazawa, 1996). Two Glu residues were found to be important for catalytic activity in the soybean  $\beta$ -amylase; Glu186 and Glu380 (Kang et al., 2004). When either of these residues were replaced activity decreased 37,000-fold (Kang et al., 2004).

The soybean  $\beta$ -amylase active site amino acids are mostly conserved with other plant species including Arabidopsis (Fulton et al., 2008). Sequence analyses of the BAM proteins in Arabidopsis revealed that BAM4 and -9 have a substitution at the Glu380 residue while BAMs1, -2, -3, -5, and -6 have the Glu380 residue (Fulton et al., 2008; Monroe, unpublished). BAM4 was confirmed to be catalytically inactive; however, there

were higher levels of starch found in a *bam4* knockout mutant versus the WT (Fulton et al., 2008) suggesting BAM4 is functional.

Sequence analysis also aided researchers in identifying localization signals on the BAM genes. About 90% of the  $\beta$ -amylase activity in Arabidopsis leaves is found outside of the chloroplasts (Lin et al., 1988; Laby et al., 2001). The protein responsible for this activity was cloned (Monroe and Preiss 1990) and the protein was identified as BAM5 and found to be prevalent in the phloem (Wang et al., 1995). Recently, BAM5 was found to be localized in the cytosol in Arabidopsis, which was expected because BAM5 does not have an N-terminal localization signal (Marafino and Monroe, unpublished).

Interestingly, the function of BAM5 is still unknown. BAM3, however, does have an N-terminal extension with characteristics like a chloroplast transit peptide signal and Lao et al. (1999) found that BAM3 was indeed localized in the stroma of the chloroplasts of pea plants using a GFP fusion protein. As well, Fulton et al. (2008) showed that BAM1, -2, -3, and -4 were all localized in the chloroplasts and Zeeman (personal communication) found that BAM6 and -9 are also localized in the chloroplast. Because BAM1, -2, -3, and -4 were all found to be in the chloroplasts, there was an initial prediction that they have a similar function (Fulton et al., 2008). However, BAM1 has been shown to be regulated by the reduction/oxidation cycle in chloroplasts, which coincides with the day/night cycle. It is activated in a reduced environment (Sparla et al., 2006) and the expression data of BAM1 suggests BAM1 is active during the day (Diurnal, Oregon State University, <http://diurnal.cgrb.oregonstate.edu/>), which is opposite of what one would expect for an enzyme predicted to be involved in starch degradation. BAM1 has also been proposed to aid in leaf starch degradation when the plant is under certain types of

stress (Sparla et al., 2006), in particular, heat stress (Kaplan and Guy, 2004), which is more likely to occur during the day.

The  $\beta$ -amylase activity of BAM1, -2, -3 and -4 were measured and it appears that BAM1, -2, and -3 have activity but BAM4 does not (Fulton et al., 2008). A three dimensional (3D) model of BAM4 suggested a loss of catalytic capacity because differences were observed between the amino acids of the glucan binding site of BAM4 compared to the other active,  $\beta$ -amylases (BAM1, -2, and -3) (Fulton et al., 2008). *BAM7* and *BAM8* were different than the other *BAM* genes in that they contain an extension of ~150 amino acids on the N-terminus (Fulton et al., 2008). The proteins these genes code for were recently localized by creating transgenic Arabidopsis plants expressing BAM-GFP fusion proteins (Zeeman, personal communication; Monroe unpublished). It was discovered that both of these proteins are localized in the nucleus. The N-terminal extension of BAM7 and -8 contain a basic helix-loop-helix DNA binding domain (Reinhold, personal communication) and are believed to have a role in regulating transcription.

Even though the BAM proteins have different functions it appears that the  $\beta$ -amylase proteins depend on one another to function. Some of the BAM proteins seem to have larger roles in starch degradation than others, and starch accumulation seems to increase when those genes are paired in double knockout mutant plants. Fulton et al. (2008) measured the levels of starch in single, double, triple and quadruple knockouts of BAM genes in Arabidopsis. This is an example of  $\beta$ -amylase proteins working together, in particular the *bam1,3* knockout. The *bam1* knockout plants did not affect starch break down as much as *bam3*, but the double knockout showed a more severe phenotype than

the single knockouts together (Fulton et al., 2008). In the same study the starch content was measured in wild-type, *bam3* and *bam4* single mutants and *bam3,4* double knockout mutant plants and again the double mutant showed a more severe phenotype than the single knockouts.

The previous results have led researchers to believe that BAM3 is the dominant contributor to starch degradation in the chloroplasts. Also, BAM3 expression is the opposite of BAM1 expression. BAM3 expression seems to increase at night and also when plants are exposed to cold temperatures (Kaplan and Guy, 2005), while microarray analysis showed BAM1 had increased expression during heat shock, osmotic, and oxidative stress (Sparla et al., 2006). It was from these findings that the researchers concluded that BAM1 is important in starch degradation more so when BAM3 is knocked out because when the *bam1* knockout had a less severe phenotype than the *bam1,3* knockout (Fulton et al., 2008). Recently BAM3 and BAM1 were shown to be phosphorylated (Lohrig et al., 2009 and Hazlewood et al., 2008) which may influence their activity by either activating or deactivating the enzymes.

*Does BAM9 have a role in starch metabolism?*

The function of *BAM9* is unknown. Fulton et al. (2008) described differences between the Arabidopsis *BAM9* amino acid sequence and the rest of the Arabidopsis BAMs. They noted that the active site amino acids were not conserved, specifically Glu186 and Glu380. These two amino acids were shown to be important in the catalytic activity of  $\beta$ -amylases (Kang et al., 2004). Also, Fulton et al. (2008) stated that the



flexible loop that is involved in the release of a maltose after catalysis is reduced in size in BAM9.

Not only is the amino acid sequence found to be different in BAM9 from the other  $\beta$ -amylases but *BAM9* has a peak of expression at the night/day transition (Chandler et al., 2001; Smith et al., 2004) (Figure 2). This suggests that the protein may only be present when starch is accumulating, a pattern opposite of what one would expect from a protein involved in starch degradation (Fulton et al., 2008). This is unexpected because one would assume a protein involved in starch degradation would function at night, when the majority of starch degradation is occurring.

Even though the amino acid sequence suggests inactivity with starch, Chandler et al. (2001) proposed that BAM9 may be acting on different substrates. No BAMs are known to act on maltooligosaccharides, such as maltotriose. Currently the only enzyme known to remove maltotriose is Disproportionating enzyme (D-enzyme, DPE1). This enzyme is a plastidial  $\alpha$ -1, 4-glucanotransferase (Critchley et al., 2001). In the Critchley et al. (2001) study D-enzyme was suggested to aid in the metabolism of Malto-oligosaccharides (MOS) in Arabidopsis, such as maltotriose (Critchley et al., 2001). Critchley concluded that D-enzyme is involved in the breakdown of starch by synthesizing MOS molecules into larger polymers which will allow for other starch metabolites such as  $\beta$ -amylases to degrade them further. Interestingly, the expression of *BAM9* was found to be the opposite that of *D-enzyme* (Figure 3). Because *BAM9* and *D-enzyme* have opposite patterns of expression and BAM9 is likely unable to bind to starch with a reduced flexible loop (Fulton et al., 2008), it could be helping the plant degrade the smaller glucan polymers, such as maltotriose, when D-enzyme is not being expressed.

We therefore proposed that BAM9 could play a role in the breakdown of the maltotriose that has been cleaved from metabolizing starch molecules. In this study this hypothesis was investigated by testing wild-type, *bam9*, *bam3*, and *bam3,9* T-DNA insertion mutant plants for starch accumulation phenotypes and amylase activity. As well, to further test our hypothesis, the BAM9 protein was purified and tested for catalytic activity with starch and smaller oligosaccharides.

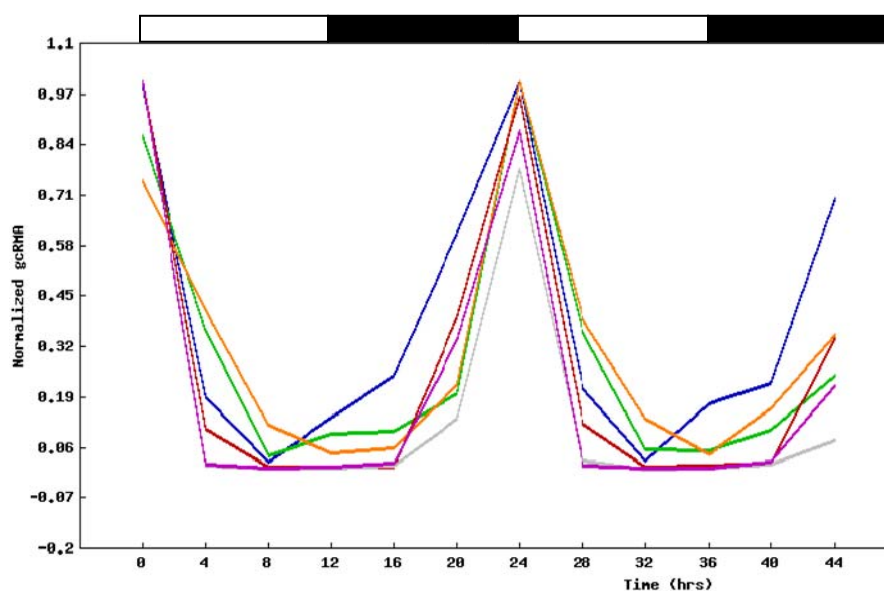


**Figure 2.** Expression data for *BAM9*. This image was generated using the Diurnal tool from Oregon State University (<http://diurnal.cgrb.oregonstate.edu/>), with six independent microarray experiments normalized onto the same graph. The six conditions are: all light (100  $\mu$ E and 22°C), 12/12 hr light/dark (100  $\mu$ E and 22°C), 16/4 hr light dark (90  $\mu$ E and 22°C), 4/16 hr light/dark (180  $\mu$ E and 22°C), 12/12 hr light/dark (130  $\mu$ E and 22°C), and 12/12 hr light/dark (180  $\mu$ E and 20°C). The white bars on top of the figure represent the light periods and the black bars represent the dark periods.

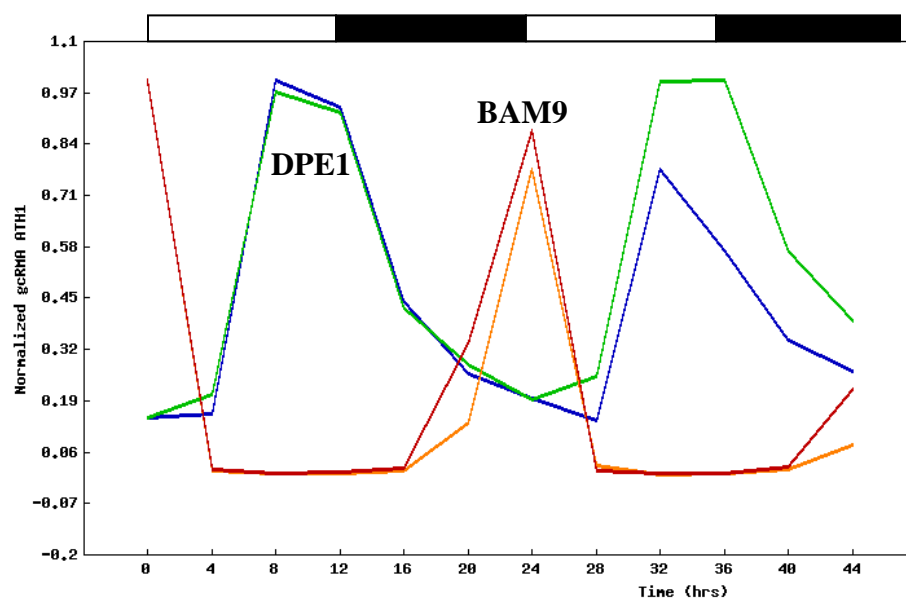


**Figure 3.** A comparison of the expression data of *BAM9* and Disproportionating Enzyme1 (D-enzyme, DPE1) in two independent microarray experiments. The experimental conditions are: 12/12 hr light/dark (130  $\mu$ E and 22°C) and 12/12 hr light/dark (180  $\mu$ E and 20°C). This graph was generated using the Diurnal tool from Oregon State University (<http://diurnal.cgrb.oregonstate.edu>) by putting the diurnal cycles of both the *D-enzyme* and *BAM9* expression data together. The white bars on top of the figure represent the light periods and the black bars represent the dark periods.

## METHODS

### Sequence Analysis and 3-D Modeling

All BAM amino acid sequences were obtained from the NCBI website (<http://www.ncbi.nlm.nih.gov/>) (Table 1). The sequences were aligned using a ClustalW2 program (<http://www.ebi.ac.uk/Tools/clustalw2/index.html>). The structure of BAM9 was modeled using the threading program PHYRE using the soybean  $\beta$ -amylase as a model (Kelley and Sternberg, 2009).

### Plant Material

Seeds were planted in 5 inch diameter pots in Horticulture Inc. Germination Mix 3 soil with nutrient solution (2.5 mM  $\text{KH}_2\text{PO}_4$ , 5 mM  $\text{KNO}_3$ , 2 mM  $\text{Ca}(\text{NO}_3)_2$ , 2.5 mM EDTA Ferric Sodium Salt, 70  $\mu\text{M}$   $\text{H}_3\text{BO}_3$ , 14  $\mu\text{M}$   $\text{MnCl}_2$ , 0.5  $\mu\text{M}$   $\text{CuSO}_4$ , 1  $\mu\text{M}$   $\text{ZnSO}_4$ , 0.2  $\mu\text{M}$   $\text{Na}_2\text{MoO}_4$ , 10  $\mu\text{M}$   $\text{NaCl}$ , 0.01  $\mu\text{M}$   $\text{CoCl}_2$ , and 2  $\mu\text{M}$   $\text{MgSO}_4$ ) and were grown under a 12/12 hr light/dark cycle. The plants were grown under 50  $\mu\text{M}\cdot\text{M}^{-2}\cdot\text{S}^{-1}$  light at 25°C. The *Arabidopsis thaliana* wild-type seeds (Columbia) and the single T-DNA insertion mutants were obtained from Arabidopsis Biological Resource Center (Ohio State University). The double BAM knockouts were generated in the Monroe lab by Lauren Saunders using standard techniques.

### Starch Quantification

The protocol provided by Smith and Zeeman (2006) was used as a guide for the following procedures. Leaves from 5 or 7 week old wild-type (WT), *bam3*, *bam9* and *bam3,9* were harvested at 8 AM or 8 PM. About 2.4 g of leaves were separated into six

**Table 1.** Accession Numbers and Gene names for  $\beta$ -amylases used in this study.

Species	$\beta$ -amylase	Accession Number	Gene Names
<i>Arabidopsis thaliana</i>	AtBAM1	NP_189034.1	AT3G23920
	AtBAM2	NP_191958.3	AT4G00490
	AtBAM3	NP_567523.1	AT4g17090
	AtBAM4	NP_568829.2	AT5G55700
	AtBAM5	NP_849389.1	AT4G15210
	AtBAM6	NP_180788.2	AT2G32290
	AtBAM7	NP_182112.2	AT2g45880
	AtBAM8	NP_001032014.1	AT5G45300
	AtBAM9	NP_197368.1	AT5G18670
<i>Populus trichocarpa</i>	PtBAM1a	XP_002314522	
	PtBAM1b	XP_002311706	
	PtBAM2	XP_002320794	
	PtBAM3a	XP_002329547	
	PtBAM3b	XP_002326690	
	PtBAM5	XP_002327920	
	PtBAM7	XP_002302584	
	PtBAM8	XP_002304400	
	PtBAM9	XP_002312750.1	
	PtBAMXa	XP_002304568	
	PtBAMXb	XP_002297961	
<i>Oryza sativa</i> (var. japonica)	OsBAM1a	NP_001064798	
	OsBAM1b	NP_001048926	
	OsBAM3	NP_001065418	
	OsBAM6	NP_001059906	
	OsBAM7	EEE70265	
	OsBAM9a	NP_001060573	
	OsBAM9b	NP_001050116	
	OsBAMX	NP_001042531	
<i>Vitis vinifera</i>	VvBAM1	XP_002285569	
	VvBAM2	XP_002282871	
	VvBAM3	XP_002282871.1	
	VvBAM4	XP_002265698	
	VvBAM5	XP_002281003	
	VvBAM7	XP_002273843	
	VvBAM8	XP_002270680	
	VvBAM9	XP_002276777.1	
	VvBAM9	XP_002276777	
	VvBAMX	XP_002263816	
	<i>Ricinus communis</i>	RcBAM9	XP_002516865.1
RcBAM3		XP_002517513.1	
<i>Glycine max</i>	GmBAM3	CAI39244.1	
	GmBAM9	CAI39245.1	
<i>Solanum tuberosum</i>	StBAM3	AAK84008.1	
	SIBAM9	CAH60892.1	
<i>Solanum lycopersicum</i>	SIBAM9	CAH60892.1	

Common names: Poplar (*Populus trichocarpa*), Castorbean (*Ricinus communis*), Grape (*Vitis vinifera*), Soybean (*Glycine max*), Potato (*Solanum tuberosum*), Tomato (*Solanum lycopersicum*), and Rice (*Oryza sativa*)

replicates containing ~0.4 g each. The samples were immediately stored at -80°C until needed for further processing.

Five mL of 80% ethanol were added and each sample was placed in a 100°C boiling water bath for 3 min. The samples were centrifuged for 8 min at 3,000 rpm and the ethanol was discarded and 5 mL more of ethanol was added. The boiling and centrifuge steps were repeated two more times, then samples were stored in a -80°C freezer. Each sample of leaves was homogenized using a mortar and pestle with 1 mL aliquots of deionized H<sub>2</sub>O until the final amount of homogenate reached 5 mL. After homogenization, 500 µL of each sample was transferred to four screw cap microcentrifuge tubes, and then 500 µL of 200 mM Na acetate, pH 5.5 was added to each sample. To half of the samples the enzymes α-amylase (0.5 U) and α-amylglucosidase (6 U) were added. The other half received an equal volume of deionized H<sub>2</sub>O. All samples were then placed in a 37°C incubator for ~4 hrs and then stored at -20°C until the glucose was assayed.

For the glucose assay, each sample contained a final volume of 1 mL with 100 mM HEPES (pH 7.5), 0.5 mM ATP, 1 mM NADP, 4 mM MgCl<sub>2</sub> and 50 µL of the starch digest sample. To start the reaction, 1 µL of a 1 U/µL hexokinase-glucose 6-phosphate dehydrogenase solution (HK-G6PD) or 2 µL of 5 U/µL HK and 2 µL of 3.85 U/µL G6PD were added to each sample. Assays were allowed to run for at least 10 minutes and no more than 1 hr. The absorbance was read at 340 nm.

## **Amylase Assays**

### *Harvest and Homogenization*

Mature leaves were harvested between 0-1 hr after the light or dark phase began. The plants were 5-8 weeks old when harvested. About 1 g of leaf material was immediately frozen in a -20°C freezer until all samples were harvested. Each leaf sample was then cut using a razor blade and the pieces were divided into three replicates. Each of the replicates was homogenized in four volumes of buffer (50 mM 3-[N-Morpholino] propanesulfonic acid (MOPS, pH 7.0) and 5 mM DL-Dithiothreitol (DDT)) using a mortar and pestle. The homogenized tissue was then centrifuged at 13,000 rpm for 10 min at 4°C and the supernatant was transferred to a clean 1.5 microcentrifuge tube.

### *Amylase Assay*

The crude extracts were assayed in triplicate with one control sample. The assays were run in an assay buffer containing 5 mg/mL starch and 50 mM MOPS, pH 7.0. For each assay 50 µL of the diluted crude extract was used to start the reaction. The assays were run at 37°C for 30 min and stopped by placing the samples in a boiling water bath (100°C) for ~2 minutes.

Reducing sugars were then quantified using the procedure of Nelson (1944). Five-hundred µL of Copper A (230 mM Na<sub>2</sub>CO<sub>3</sub>, 85.5 mM Rochelle Salt, 287.5 mM NaHCO<sub>3</sub>, and 170 mM Na<sub>2</sub>SO<sub>4</sub>) and Copper B (600 mM CuSO<sub>4</sub>·5 H<sub>2</sub>O, 200 mL water with 4 drops of concentrated H<sub>2</sub>SO<sub>4</sub>) reagents in a 25:1 ratio were added to each sample which were then placed in a boiling water bath (100°C) for 15 min. Five-hundred µL of Arsenomolybdate (257 mM Ammonium Molybdate, 42 mL concentrated H<sub>2</sub>SO<sub>4</sub>, and 22.5



mM Na<sub>2</sub>HAsO<sub>4</sub>·7 H<sub>2</sub>O) was added to each sample and vortexed. Each sample then received 3 mL of deionized H<sub>2</sub>O, was inverted to mix and centrifuged for 3 min at 2000 rpm. The absorbance was read at 660 nm.

### *Protein Assay*

The Bio-Rad protein assay protocol was used. Five standards of Bovine Serum Albumin (BSA) were run in duplicate along with the samples. Each sample was diluted with H<sub>2</sub>O to final volume of 20 µL. The Bio-Rad Protein Assay Dye Reagent Concentrate was diluted in a 1:5 ratio with deionized H<sub>2</sub>O. One mL of the diluted solution was used for each assay. The samples were incubated at room temperature for ~1 hr and then the absorbance was read at 595 nm.

## **Measuring mRNA**

### *Extraction of RNA*

Leaf material was harvested between 5 and 8 weeks of age at various times of day. About 0.3 g of leaf material was placed in liquid nitrogen and homogenized using a mortar and pestle treated with RNase Free Zap Wipes or the leaf material was placed in the -80°C freezer for at least 24 hr. The mortar and pestle was kept in a -20°C freezer before homogenizing if the leaves were stored at -80°C.

Homogenized material was vortexed with 10 volumes of Tri Reagent (Ambion) and incubated at room temperature for 5 min. To each sample, 200 µL of chloroform per mL of Tri Reagent was added and mixed by shaking for ~20 s. The samples were again incubated at room temperature for 5 min and then centrifuged for 15 min at 12,000 x g at

4°C. Then the aqueous phase was transferred to a new tube where 500  $\mu$ L of isopropanol per mL of Tri Reagent was added and vortexed, and then incubated for 5 min at room temperature. Samples were then centrifuged for 8 min at 12,000 x g at 4°C. The supernatant was discarded and an equal volume of 75% ethanol was added to each sample. Samples were then centrifuged at 7,500 x g for 5 min at 4°C. The remaining ethanol was discarded and the samples were centrifuged for an additional minute. Again the ethanol was discarded and the samples were dried under a fume hood for 2 min. Sixty  $\mu$ L of Nuclease-free sterile H<sub>2</sub>O was added to each sample which was then treated using the Turbo DNA-free Kit (Ambion). Seven  $\mu$ L of DNA-free buffer and 1  $\mu$ L of DNase was added to each sample and incubated at 37°C for 30 min. Another 1  $\mu$ L of DNase was added and the samples were again incubated at 37°C for 30 min. After incubation, 7  $\mu$ L of DNase inactivation reagent was added to the solution and allowed to sit at room temperature for 5 min with occasional tapping to resuspend the inactivation reagent. The samples were centrifuged at 13,000 rpm for 1.5 to 3 min and the supernatant was transferred to a new RNase-free microcentrifuge tube. The concentration and purity of RNA was measured using a Nano-Drop spectrophotometer in duplicate at 260 nm and 280 nm. No RNA samples with purities outside of the range of A260/A280 of 1.8-2.1 were used in the following experiments. The RNA was stored at -20°C.

#### *Reverse Transcription and Polymerase Chain Reaction*

The iScript protocol (BioRad) was used to synthesize cDNA from the extracted RNA. Oligo (dT) primers were used to amplify the mRNA. Four  $\mu$ L of 5X iScript select reaction mix, 1  $\mu$ L of iScript reverse transcriptase, 2  $\mu$ L of Oligo (dT) primer, and 1  $\mu$ g of

total RNA was used in each reverse transcription reaction. To make the total volume of the reaction mix 20  $\mu$ L, Nuclease-free sterile H<sub>2</sub>O was added when necessary. The samples were incubated at 42°C for 60-90 min, 85°C for 5 min, and then 4°C until samples were stored at -20°C.

The synthesized cDNA was used as the template for PCR with Arabidopsis  $\beta$ -amylase primers. Primers for semi-quantitative and Real-Time PCR were generated using the NCBI Primer-BLAST Primer designing tool. The resulting primers were then checked for self and pair dimers as well as hair-pin loops using DNASTar. The nucleotide sequences for the Actin2 primers were obtained from Charng et al. (2006). All of the primers used in this study can be seen in Table 2. Both semi-quantitative PCR and Real-Time PCR were used in this study to quantify the expression of the chosen genes. Table 3 shows the heating sequence used for semi-quantitative PCR and Table 4 shows the heating sequence for Real-Time PCR.

### **Protein Purification of BAM3 and BAM9**

The following procedures for purification were performed by Kevin Fedkenheuer, John Herlihy, and Dr. Jonathan Monroe.

#### *Generating Recombinant Plasmid*

WT RNA was extracted and reverse transcribed using the methods described above. The full-length-*BAM9* and *BAM3* cDNAs were amplified using the following primers: *BAM3*-F, 5' AGGATCCACACGTTCTCTCAT ACCCACAC 3', *BAM3*-R, 5' AGGTCGACTTACTACTAAAGCAGCCTCCTC, *BAM9*-F, 5' TAGTTTGCAAACC

**Table 2.** Primers used for semi-quantitative and Real-Time PCR.

<b>Target Gene</b>	<b>Small Product Primers (5'-3')</b>
<b><u>Actin2</u></b>	
Forward	GACCTTGCTGGACGTGACCTTAC
Reverse	GTAGTCAACAGCAACAAAGGAGAGC
<b><u>L23a</u></b>	
Forward	GCAAAGGCTGTGAAGTCTGG
Reverse	GAGTAGCGCTGATTTTTGGG
<b><u>BAM3</u></b>	
Forward	TGCGAAGATGAAGCCGCCAAC
Reverse	GTCGTTCTTGGAGTGTGGGT
<b><u>BAM9</u></b>	
Forward	CCAAATCCATAATCCTCACCA
Reverse	CTCTGCAGATCCTCGCTTG
	<b>Whole Gene Product Primers (5'-3')</b>
<b><u>BAM3</u></b>	
Forward	GGGAATTCATGGAATTGACACTGAATTCCTCG
Reverse	ATGGATCCAACACTAAAGCAGCCTCCTCCAC
<b><u>BAM9</u></b>	
Forward	GGGAATTCATGGAAGTTTCAGTGATTGGA
Reverse	AAGGATCCATAGCGGTTTGCAAACACTAGGT

**Table 3.** Semi-quantitative PCR heating protocol.

<b>Step</b>	<b>Cycles</b>	<b>Temperature (°C)</b>	<b>Time(min)</b>
1	1	94	5:00
2	4	94	0:30
3		52	0:30
4		72	1:30
5		20-35	94
6	56		0:30
7	72		1:30
8	1	72	20:00
9	1	4	Forever

**Table 4.** Real-Time PCR protocol.

<b>Step</b>	<b>Cycles</b>	<b>Temperature (°C)</b>	<b>Time(min)</b>
1	1	50	2:00
2	1	95	15:00
3	36	94	0:10
4		54	0:30
5		72	0:30
6	1	72	10:00
7	Melting Curve	72-95	0:20 each degree
8	1	72	10:00
9	1	4	Forever

GCTTAAGTCGACGG 3', and *BAM9-R* 5'CCGTCGACTTAAGCGGTTTGCAAACCTA 3'. The PCR products were then cloned into pETduet-1 (Invitrogen) which generates a six-His tag at the protein's C-terminus. Both the vector pETduet-1 and the PCR products were cut with restriction enzymes *Bam*H1 and *Sal*1. After ligation the recombinant plasmids were transformed into the cloning strain of *E. coli* (DH5 $\alpha$ ). After growth over night in LB media, the plasmid DNA was minipreped and sent to MWG/operon for sequencing.

#### *Transformation of BL21 cells and Protein Purification*

The BAM9 and BAM3 plasmids were transformed into BL21 cells by rapid colony transformation (Micklos and Freyer, 1990). However, after preliminary protein expression experiments we realized that BAM3 did not express well so we checked for rare codons using the Rare Codon Calculator, ([www.doe-mbi.ucla.edu/~sumchan/caltor.html](http://www.doe-mbi.ucla.edu/~sumchan/caltor.html)). This indicated that BAM3 contained 74 rare codons of 491 total codons of which 8 were found to be consecutive in the nucleotide sequence. This suggested possible problems in the rate of BAM3 translation and so BAM3 was expressed in the BL21-CodonPLUS *E. coli* strain to help increase its expression. Cells were grown in 250 mL of LB broth with 80  $\mu$ g/mL carbenicillin. The cells were grown in a 22°C incubator shaking at 250 rpm until an O.D. of 0.9 was reached. The cells were then induced with 1 mM IPTG and grown again at 22°C, shaking at 250 rpm for 18-22 hours. After incubation, the cells were centrifuged at 4000 x g for 10 min. The supernatant was discarded and the cell pellet was resuspended in 25 mL of TE buffer (10 mM Tris and 1 mM EDTA). The cells

were then sonicated using a Misonix Ultra Liquid Processor for five, 10 s bursts at 40% intensity. The samples were incubated on ice for 1.5 min between each sonication burst.

Because BAM9 was expected to be catalytically inactive, an activity assay could not be used to follow its purification and therefore co-purification with BAM3 was performed to design a purification method that would yield presumably-functional BAM9 protein. After sonication, the BAM3 soluble fraction was assayed for activity via an amylase assay as described above. After BAM3 activity was confirmed, the samples were incubated with Talon Metal Affinity Resin (Clontech). The proteins were purified using equilibration/wash buffer (50 mM sodium phosphate, 300 mM NaCl, pH 7.0) and elution buffer (50 mM Sodium Phosphate, 300 mM NaCl, and 150 mM Imidazole, pH 7.0). Samples were separated on 10% SDS polyacrylamide gels and stained with coomassie blue. Amylase activity with starch was measured for both pure BAM3 and BAM9 using methods described above.

#### *Thin Layer Chromotography (TLC)*

In order to assay the activity of BAM9, pure BAM3 and -9 were incubated with various maltooligosaccharides. Substrates of 0.25% (w/v) maltotriose, maltohexose and maltopentose were mixed with a 50 mM MOPS buffer (pH 7) and 2.31  $\mu$ g of pure BAM9 or 0.78  $\mu$ g of pure BAM3 at 37°C for 50 min. Samples were incubated with or without 2 mM DTT. Standards of 0.5 % (w/v) glucose, maltose, maltotriose, maltotetrose, maltopentose, and maltohexose were used. After incubation, standards and each assay mixture were spotted onto a TLC plate (Whatman 250  $\mu$ m layer aluminum-backed Silica gel plates). A butanol:ethanol:water (2:1:1) solvent ascended the TLC plate. After the



solvent front ran to the top of the TLC plate, the plate was allowed to dry and was sprayed with 10% acetic acid in methanol. The plates were again allowed to dry, and then they were incubated at 100-150°C for 10 min or until dark spots were observed.

## RESULTS

### *Phylogenetic Analysis of Arabidopsis $\beta$ -amylases*

There are nine  $\beta$ -amylase genes (BAMs) in *Arabidopsis thaliana*. The amino acid sequences of these BAMs were aligned with the homologous amino acid sequences from poplar (eleven), grape (nine), and rice (eight). Once aligned a phylogenetic tree was generated (Figure 4). The protein numbers follow the numbering system of the Arabidopsis BAMs. This phylogenetic analysis suggests six  $\beta$ -amylases were found in the ancestral plant before the monocot/eudicot separation. The six main groups found include: BAM2, -7, and -8, BAM5 and -6, BAM1, BAM3, BAM9 and one group labeled “X” because it did not contain an Arabidopsis ortholog. It is not known whether a BAM4 ortholog ancestor existed before the separation. Grape orthologs were found in every clade but this is not the case for poplar and rice. Rice orthologs are missing in the BAM2 and -8 clades and poplar orthologs are missing in BAM4 and -6 clades. Interestingly, the BAM9 group include all of the species in this study.

### *Sequence Analysis and 3-D Modeling*

The catalytically active soybean BAM was crystallized and modeled and the amino acids in the active site were identified (Mikami et al., 1993). There are fifteen amino acids found in the active site of the soybean BAM. Thirteen of them were found to hydrogen bond to the first four glucose residues of the non-reducing end of a starch molecule (Mikami et al., 1993). These residues are depicted in Figure 5 under the G1-4

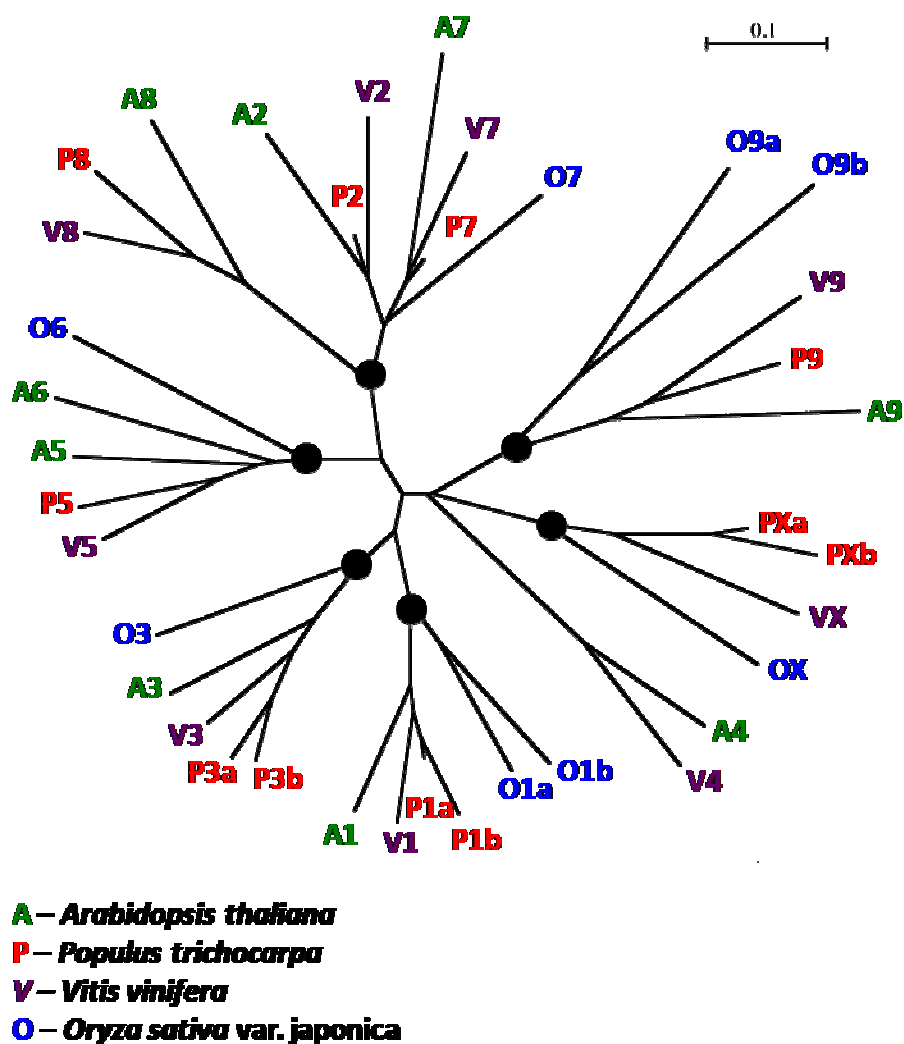


**Figure 4.** Arabidopsis BAM proteins compared to poplar, grape, and rice BAM proteins. Amino acid sequences of all BAM genes from four sequenced plant genomes were aligned using ClustalW2 (<http://www.ebi.ac.uk/Tools/clustalw2/index.html>) and a neighbor-joining tree was drawn using Unrooted (<http://pbil.univ-lyon1.fr/software/unrooted.html>). Black dots represent unique ancestral BAM genes from which descendants exist in both monocots and eudicots.

headings indicating Glucose1-4. The two amino acids in the active site that do not bind to the glucose molecules have been shown to cleave the starch molecule after the second glucose residue, releasing a maltose (Kang et al., 2004).

The active site amino acids of the active soybean BAM were compared to the Arabidopsis BAMs and found to be completely conserved with five of them, Arabidopsis BAM1, -2, -3, -5 and -6 (Figure 5). Each of these proteins is known to be catalytically active (Monroe and Priess, 1990; Fulton et al., 2008; and Zeeman, personal communication). The 15 active site amino acids of the Arabidopsis BAM9 were also aligned with BAM9 orthologs from poplar, castorbean, grape, soybean, tomato, and apricot (Figure 5). Only seven of the fifteen amino acids in the soybean BAM active site are conserved in BAM9. However, most of the active site amino acids are conserved between the BAM9 orthologs excluding four amino acids binding in the third glucose (G3) binding site (Figure 5). The BAM9 orthologs are completely conserved at the first and second glucose binding sites (G1 and G2) and the site at which maltose would be cleaved. Also, D101, one of the active site amino acids in the active soybean BAM, is missing in all of the BAM9 orthologs (Figure 5). This amino acid is in a set of five amino acids found in the flexible loop of the binding site of the soybean  $\beta$ -amylase (Figure 6). As well, when D101 was substituted in the catalytically active soybean BAM all activity was lost (Totsuka et al., 1994).

Because BAM9 was shown to be localized in the chloroplast (Zeeman, personal communication) and BAM3 is suggested to comprise the majority of the amylase activity found in the chloroplasts (Fulton et al., 2008), BAM9 orthologs were aligned with BAM3 orthologs in order to search for residues conserved only in BAM9 that might suggest

unique functions. Twenty-four amino acid residues were found to be perfectly conserved in the BAM9 orthologs that are different in the BAM3 orthologs (data not shown) (Herlihy and Monroe, unpublished). Using the BAM9 amino acid sequence, the threading program PHYRE (Kelley and Sternberg, 2009) generated a BAM9 hypothetical 3D model based on the previously crystallized active soybean BAM structure (Mikimi et al., 1993) (Figure 7). This 3D-model shows that some of the 24 conserved residues are located in the putative active site, and may bind to a ligand. Two cysteines that are in close proximity to one another, C320 and C353, are conserved in BAM9 (Figure 7) and may form a disulfide bridge. Also, the 3D-model revealed that a group of the conserved residues occur in cluster on the outside of the molecule (Figure 7) including hydrophobic amino acids, suggesting a novel binding site.

### *Starch Quantification*

*bam9* and *bam3* T-DNA insertion mutants were obtained from Stalk Institute. The insertions were confirmed using PCR (data not shown). In addition, the *bam9* T-DNA insertion mutant was confirmed by semi-quantitative PCR measuring the expression of the *BAM9* gene. This was done by using cDNA templates generated from reverse transcribed RNA extracted from both the WT and *bam9* mutant plants (Figure 8). Double knockout mutants were generated by Lauren Saunders in the Monroe Lab using standard methods.

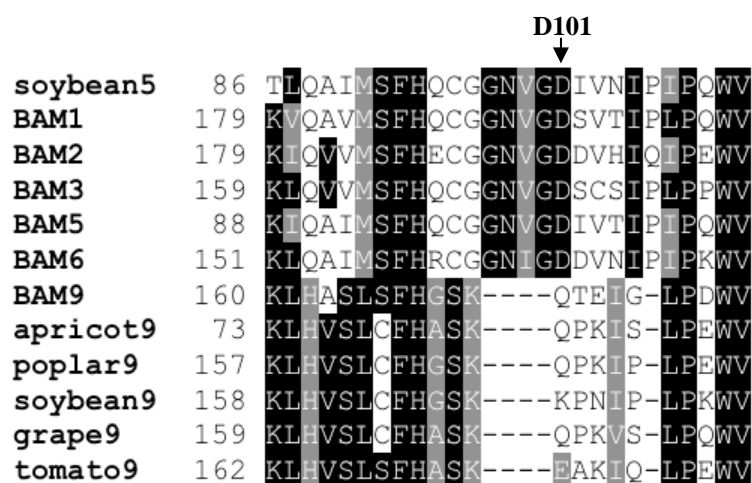
Preliminary iodine staining experiments were performed to test whether BAM9 had a starch accumulation phenotype (Figure 9). Leaves from WT, *bam3*, *bam9* and *bam3,9* knockout mutants were harvested at the end of the night when the starch content

	Terminal maltose							Penultimate maltose								
	G1				G2			G3					G4			
<b>Soybean</b> <sup>1</sup>	D53	H93	D101	R420	K295	N381	A382	E186	E380	R188	Y192	G298	F341	T342	H300	
BAM1	D	H	D	R	K	N	A	E	E	R	Y	G	F	T	H	active <sup>2</sup>
BAM2	D	H	D	R	K	N	A	E	E	R	Y	G	F	T	H	active <sup>2</sup>
BAM3	D	H	D	R	K	N	A	E	E	R	Y	G	F	T	H	active <sup>2</sup>
BAM5	D	H	D	R	K	N	A	E	E	R	Y	G	F	T	H	active <sup>3</sup>
BAM6	D	H	D	R	K	N	A	E	E	R	Y	G	F	T	H	active <sup>4</sup>
BAM9	P	H	-	R	K	N	S	E	Q	K	H	L	I	P	H	
Poplar9	P	H	-	R	K	N	S	E	Q	R	D	L	L	P	H	
Castorbean9	P	H	-	R	K	N	S	E	Q	R	H	L	L	P	H	
grape9	P	H	-	R	K	N	S	E	Q	R	H	V	L	P	H	
soybean9	P	H	-	R	K	N	S	E	Q	R	H	L	L	P	H	
tomato9	P	H	-	R	K	N	S	E	Q	R	H	L	L	P	H	
apricot9	P	H	-	R	K	N	S	E	Q	R	H	L	L	P	H	

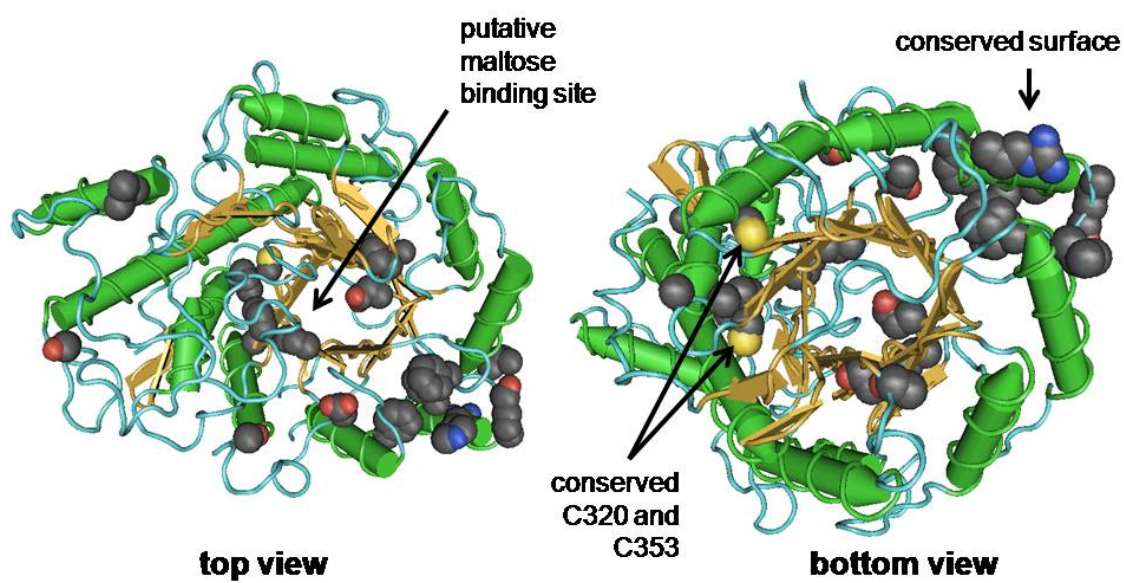
  

<span style="background-color: yellow; border: 1px solid black; display: inline-block; width: 15px; height: 10px;"></span>	soybean active site residues		<sup>1</sup> Laederach et al. 1999
<span style="background-color: lightblue; border: 1px solid black; display: inline-block; width: 15px; height: 10px;"></span>	soybean catalytic residues		<sup>2</sup> Fulton et al. 2008
<span style="background-color: cyan; border: 1px solid black; display: inline-block; width: 15px; height: 10px;"></span>	residues conserved with soybean		<sup>3</sup> Monroe et al. 1991
<span style="background-color: orange; border: 1px solid black; display: inline-block; width: 15px; height: 10px;"></span>	most common different residues		<sup>4</sup> Zeeman, personal communication
<span style="background-color: magenta; border: 1px solid black; display: inline-block; width: 15px; height: 10px;"></span>	different residues within BAM9 orthologs		

**Figure 5.** The amino acids of the  $\beta$ -amylase active site comparing five active BAMs to the BAM9 orthologs. G1, -2, -3, and -4 represents the four terminal glucose molecules of the substrate starch in which the soybean BAM binds at the reducing end. Cleavage by the soybean BAM occurs between the G2 and G3 is catalyzed by two Glutamic acid residues, E186 and E380.



**Figure 6.** A region of the amino acid sequence of the soybean  $\beta$ -amylase aligned with five active Arabidopsis BAMs and five BAM9 orthologs. A ClustalW alignment tool (Boxshade) was used to create this image. The numbers on the left of the amino acid sequence are the numbers at which the amino acid sequence starts for each species. The black represents conserved residues; the gray represents conservative amino acid changes and the white represents non-conserved amino acids.



**Figure 7.** Two views of a hypothetical 3D model of the BAM9 protein generated using the threading program PHYRE (Kelley and Sternberg, 2009) and visualized using Cn3D. The space filling amino acids are 24 residues found to be conserved within the BAM9 orthologs that are different from BAM3 orthologs.



of leaves was expected to be the lowest. The WT and *bam9* mutant leaves were a light tan. BAM3 is known to be active in starch degradation in the chloroplasts and leaves from the *bam3* mutant were a darker color. Similar results were seen by Fulton et al. (2008). Interestingly, the *bam3,9* mutant seemed to be darker than the *bam3* mutant (Figure 9).

Starch quantification was performed to confirm the iodine experiments. Two separate experiments were done with six fresh leaf replicates harvested at either 8:00 AM or 8:00 PM. Plants were harvested at five weeks of age for one experiment and seven weeks of age for the second experiment. For both experiments the WT showed more starch accumulation after the day than after the night (Figure 10). The *bam3* mutants showed more starch accumulation for harvests after the night (~2 mg more) and after the day (~1 mg more) compared to WT. The *bam9* mutants at the end of the night had ~0.5 mg more starch than WT; however, the *bam9* mutants had ~1.5 mg less starch than the *bam3* mutant (Figure 10). The *bam3,9* double mutant accumulated much more starch compared to the WT at the end of the night. The starch accumulation for the double mutant at the end of the night was ~5 mg, which was more than the sum of the single mutants, which only accumulated a sum of ~3.5 mg more starch than WT (Figure 10). Also, the difference between the starch accumulation at the end of the day and the starch accumulation at the end of the night is greater in the WT (~5 mg difference) compared to both the single knockout mutants, (~4.5 mg difference for each) and the double knockout mutant (~3.5 mg difference).

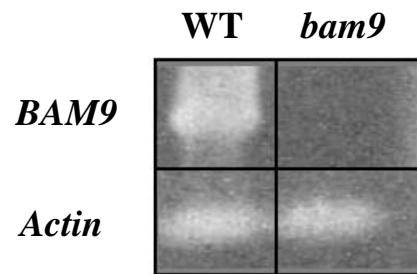


**Figure 8.** *bam9* T-DNA mutant does not show *BAM9* expression. mRNA was isolated from ~6-week-old wild-type (Columbia) and mutant plants at 9 AM, reverse-transcribed and used as template in PCR. Whole *BAM9* gene primers designed by Dr. Elizabeth Doyle and Dr. Jonathan Monroe and actin primers were from Charng et al. (2006).

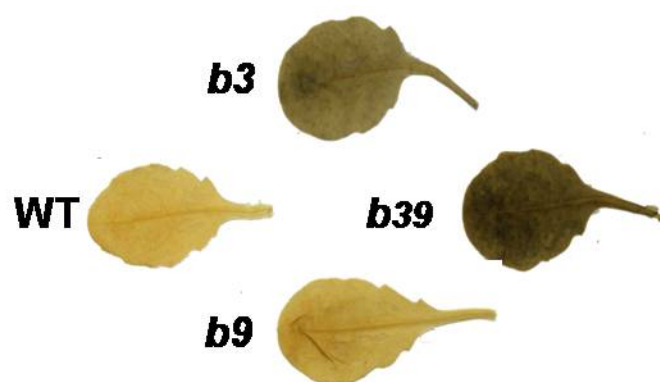


**Figure 9.** Leaves stained with iodine for starch accumulation. Leaves were harvested at the beginning of the light cycles, were boiled in 80% ethanol and then placed in iodine for about 5 min.

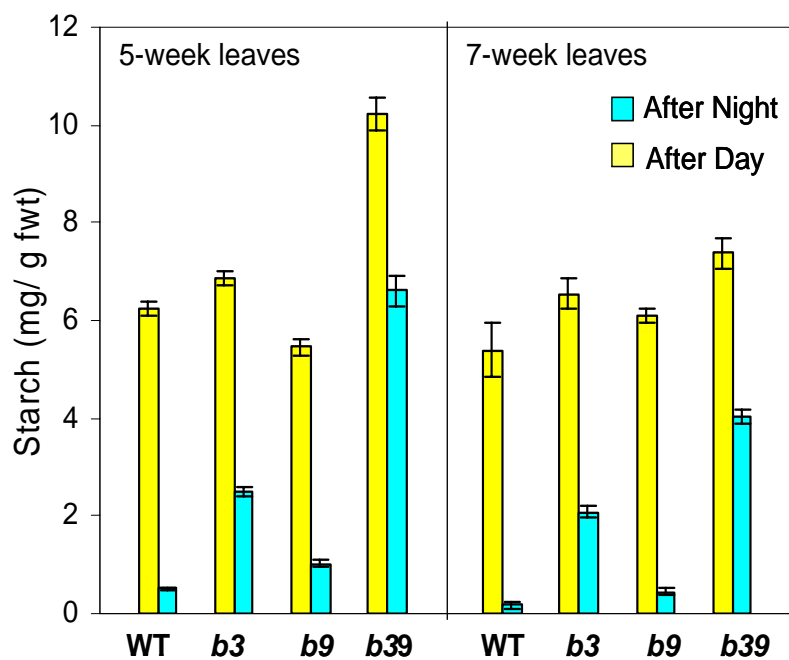


**Figure 10.** Quantification of starch in *Arabidopsis thaliana*. Measurements of samples from six independently extracted batches of plants were used for each experiment. The leaves were harvested either at end of the night (blue bars) or at the end of the day (yellow bars). The bars represent the amount of starch accumulation in grams per mg of fresh weight of leaves. Error bars represent  $\pm$  SD, n=6.

### *Amylase Assays*

Amylase assays were conducted to test whether the starch quantification phenotypes were due to the amount of amylase activity in the mutant plants. Plants were harvested between four and six weeks of age at various times of day. In amylase assays the *bam9* mutant had a greater amount of activity as compared with the WT (Figures 11 and 12). The *bam3* mutant had less activity than WT and the *bam3,9* mutant had less activity than observed in WT (Figures 11 and 12). BAM5 is catalytically active (Monroe and Priess, 1990) and is known to be localized in the cytosol (Marafino and Monroe, unpublished). Doyle et al. (2007) concluded that as leaves age BAM5 activity increases. This could be the reason for the variability in our data. It should be noted that the results in some experiment were inconsistent with the results in Figures 11 and 12. More work is needed to understand this variability.

### *The effect of BAM9 on the expression of BAM3*

The amylase assay and microarray data from the Diurnal website led us to propose that BAM9 is down regulating BAM3. This is because in the amylase assay experiments the *bam9* mutant had more than or equal activity to WT whereas the *bam3* and *bam3,9* mutants had less than or equal activity to WT suggesting that without BAM9, BAM3 may be more active. As well, the microarray data comparing the *BAM3* and *BAM9* expression data showed that as *BAM9* had a peak of expression, the expression of *BAM3* was declining (data not shown). If BAM9 normally down regulates BAM3, it could be at the level of transcription or it could be a post-translational effect.

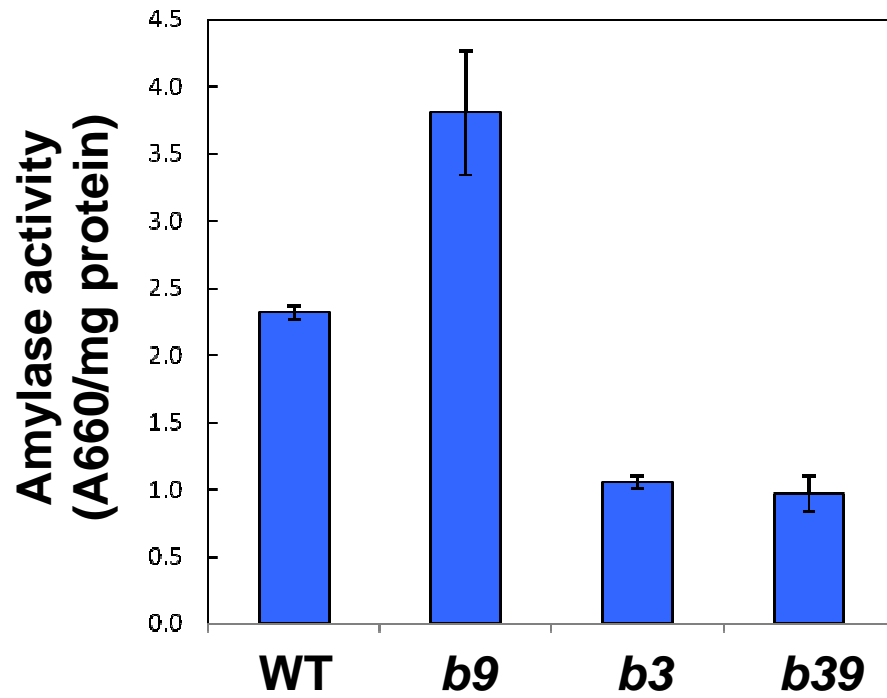


**Figure 11.** Amylase activity in crude extracts from ~5 week old leaves of WT, *bam9*, *bam3*, and *bam3,9* mutants. Starch was used as the substrate in 30 min assays. The bars represent the average A660/mg protein. Error bars represent  $\pm$  SD, n=3

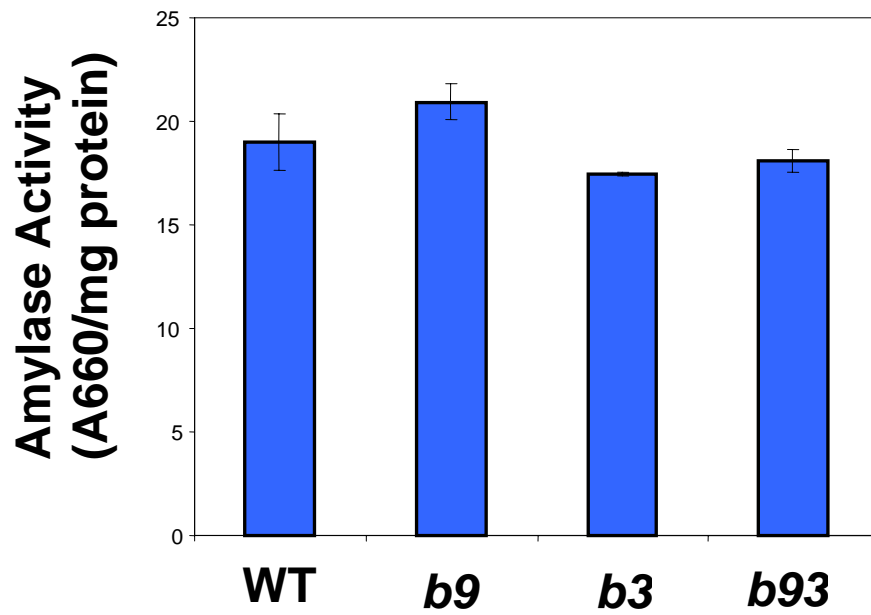


**Figure 12.** Amylase activity in crude extracts from ~6 ½ week old leaves of WT, *bam9*, *bam3*, and *bam3,9* mutants. Starch was used as the substrate in 30 min assays. The bars represent the average A660/mg protein. Error bars represent  $\pm$  SD, n=3

In order to rule out transcriptional regulation, RNA was extracted from the WT and *bam9* mutant plants to test if the BAM9 protein affects the expression of *BAM3*. The RNA was reverse transcribed into cDNA, which was then used in either semi-quantitative PCR or Real-Time Quantitative PCR (QPCR). Semi-quantitative PCR was used to test for large differences in *BAM3* expression between WT and *bam9*. PCR products after 20, 25, 30, and 35 cycles were separated on an agarose gel. Primers near the 3' end of the cDNA with a product size around 200 bp were chosen to get the most possible product amplified, as well as to be used in QPCR (Table 4). There was no apparent effect of BAM9 on the expression of *BAM3* using semi-quantitative PCR (Figure 13). QPCR was used to reveal potentially small differences in *BAM3* expression between the *bam9* mutant and WT. However, no significant difference was seen in the expression of *BAM3* in WT versus the expression of *BAM3* in the *bam9* mutant (Figure 14).

#### *Purification of BAM3 and BAM9*

In order to examine the catalytic activity or binding activity of BAM9, pure protein was necessary. Because BAM9 was expected to be inactive, an activity assay could not be used to follow its purification. Therefore we co-purified BAM9 with BAM3 in order to design a purification method that would yield presumably functional BAM9 protein. *E. coli* BL21 cells were transformed with His-tagged BAM9 and BL21-codonPLUS cells were transformed with His-tagged BAM3. Both BAM3 and BAM9 were then purified from the *E. coli* strains and, to confirm purification, non-induced whole cells, induced whole cells, the soluble fraction after sonication and the pure protein



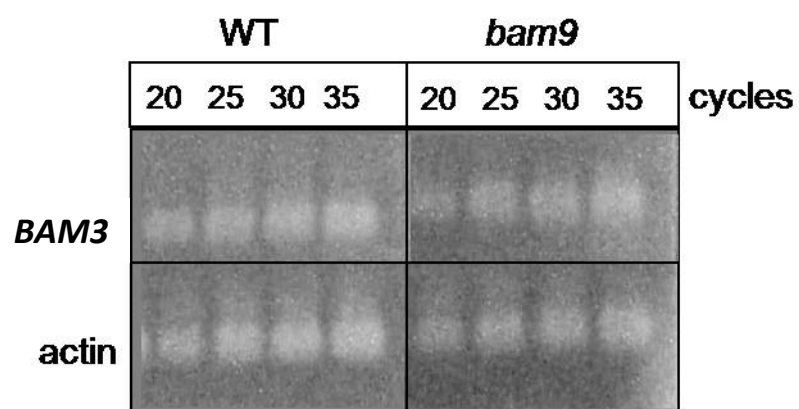


**Figure 13.** Semi-quantitative PCR comparing the expression of *BAM3* between the WT and the *bam9* mutant. mRNA was isolated from ~6-week-old wild-type (Col) and mutant plants at 9 AM, reverse-transcribed and used as template in semi-quantitative PCR. Samples were taken after 20, 25, 30, and 35 cycles. The actin primers were used as a control.

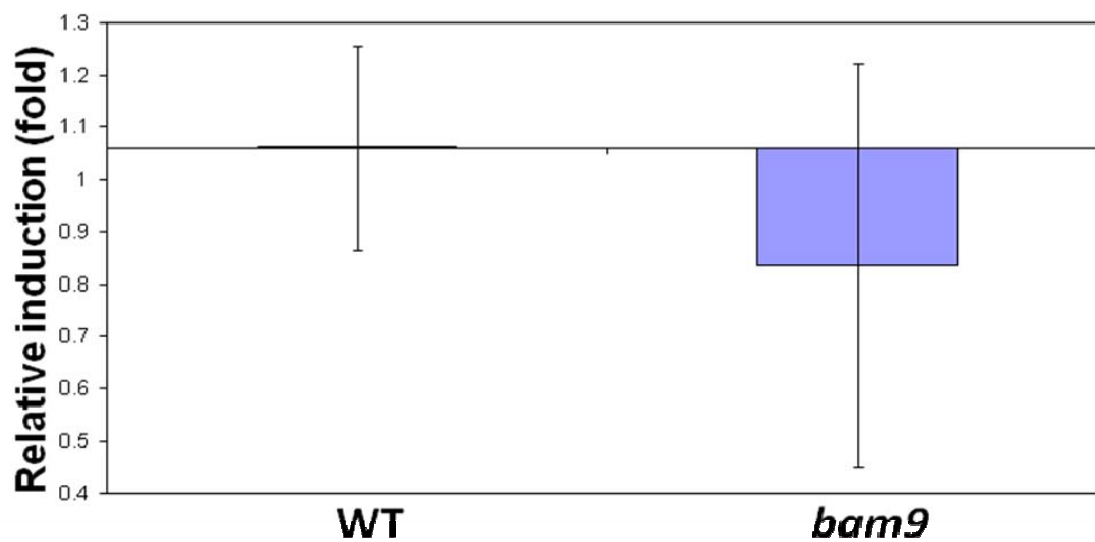


**Figure 14.** Expression of the *BAM3* gene in *bam9* mutant compared to the WT. mRNA was isolated from 6½ -week-old wild-type (Col) and mutant plants at 9 AM, reverse-transcribed and used as template in quantitative, real-time PCR. Relative *BAM3* gene expression was calculated using the comparative CT method, calibrating to the WT sample using the actin gene for normalization. Data are the average of triplicate reactions, and are from one typical experiment. Error bars indicate the standard deviation of the  $\Delta\Delta CT$  value.

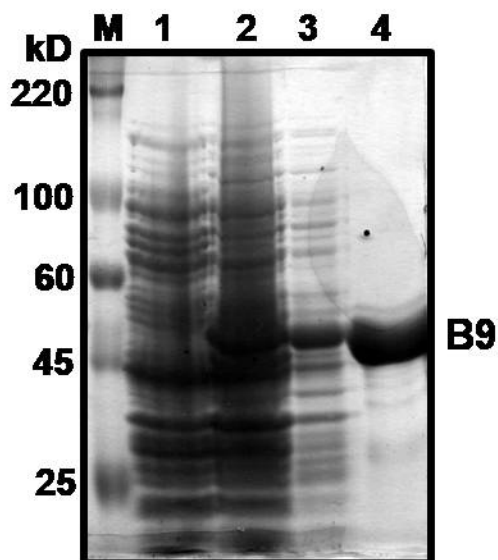


**Figure 15.** An SDS-PAGE gel of BAM9 purification. BAM9 was cloned into pETduet-1(Invitrogen) which generates a six His-tag at the protein's C-terminus. The His-tagged protein was then expressed in *E. coli* and purified. Lanes 1-4 contain pre-induced whole cells, induced whole cells, soluble fraction, and pure protein, respectively and M is the marker.

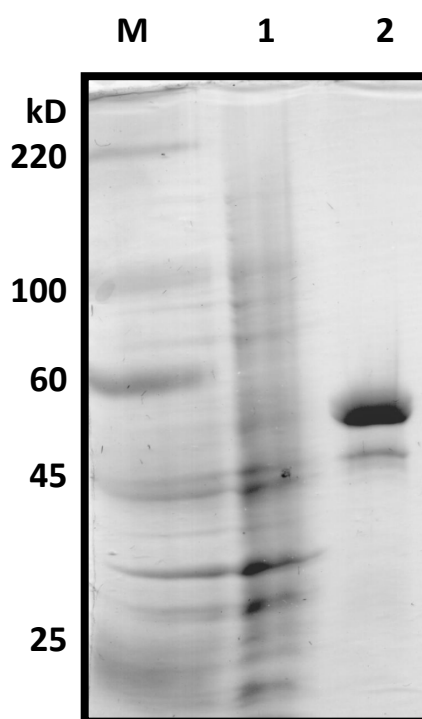


**Figure 16.** An SDS-PAGE gel of BAM3 purification. BAM3 was cloned into pETduet-1(Invitrogen) which generates a six His-tag at the protein's C-terminus. The His-tagged protein was then expressed in *E. coli* and purified. Lanes 1 and 2 contain pre-induced whole cells and pure protein, respectively and M is the marker.

were separated by SDS-PAGE electrophoresis. The expected size of BAM9 protein is 48.76 kD and the BAM9 sample of the induced whole cells showed a band at about 50 kD and the pre-induced whole cells did not show a band at about 50 kD. However, the soluble fraction of the sonicated, induced whole cells and the purified fraction did show a band at 50 kD (Figure 15). As well, the expected size of BAM3 is ~51.60 kD and Figure 15 shows the purification of BAM3 with a band at the expected position (between 50-55 kD) for the pure protein sample (Figure 16). This band was not observed in the pre-induced whole cell sample.

#### *Catalytic Activity of BAM9*

To determine whether or not BAM9 is catalytically active, pure BAM9 and BAM3 were assayed with starch. BAM3 resulted in about 9 U/mg of activity with starch whereas for BAM9 there was no detectable activity. The limit of detection was 0.01% of BAM3 activity (Figure 17). BAM3 and BAM9 were also incubated with various maltooligosaccharides. After 50 min, samples were heat-inactivated and the products were separated by thin layer chromatography (TLC). Standards allowed identification of specific products. When BAM3 and BAM9 were assayed with maltohexose the product observed on the TLC plates for BAM3 was maltose (Figures 18 and 19), whereas when BAM9 was incubated with maltohexose there was no evidence of any hydrolytic activity (Figures 18 and 19). Because BAM9 contains a pair of cysteines that may form a regulating disulfide bond (Figure 7), we included DTT in some reactions. There was no effect of DTT on the activity of either BAM3 or BAM9. BAM9 and BAM3 were also incubated with maltotriose and maltopentose. The incubation with maltotriose did not

result in hydrolysis for either protein (Figure 18). The same result occurred when BAM9 was incubated with maltopentose in which maltopentose was observed on the TLC plate. However, when BAM3 was incubated with maltopentose, maltotriose and maltose were separated on the TLC plate (Figure 19).

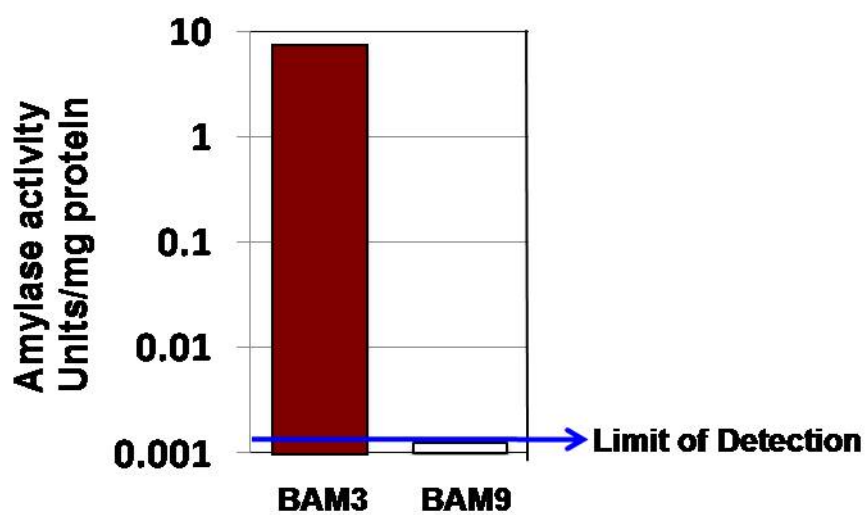


**Figure 17.** Amylase activity of BAM3 compared to the amylase activity of BAM9. Pure BAM3 and BAM9 proteins were used in amylase activity assays with starch as the substrate. The bars represent the amount of activity of the pure proteins in Units/mg.

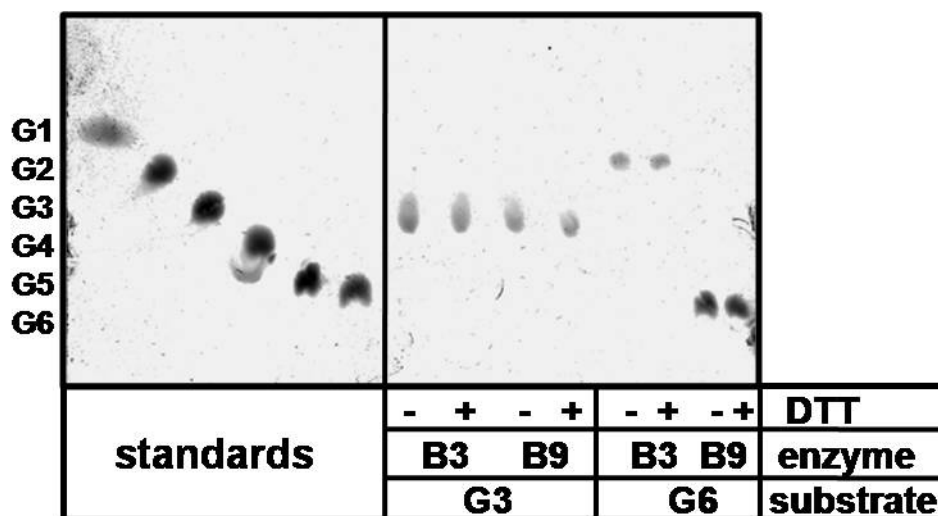


**Figure 18.** Thin Layer Chromatography of oligosaccharide products after incubation with BAM3 and BAM9. BAM3 and BAM9 were incubated with maltotriose and maltohexose for 50 min and heat-inactivated. The products were then separated on a TLC plate. G1-G6 represent the number of glucose residues within the oligosaccharide.



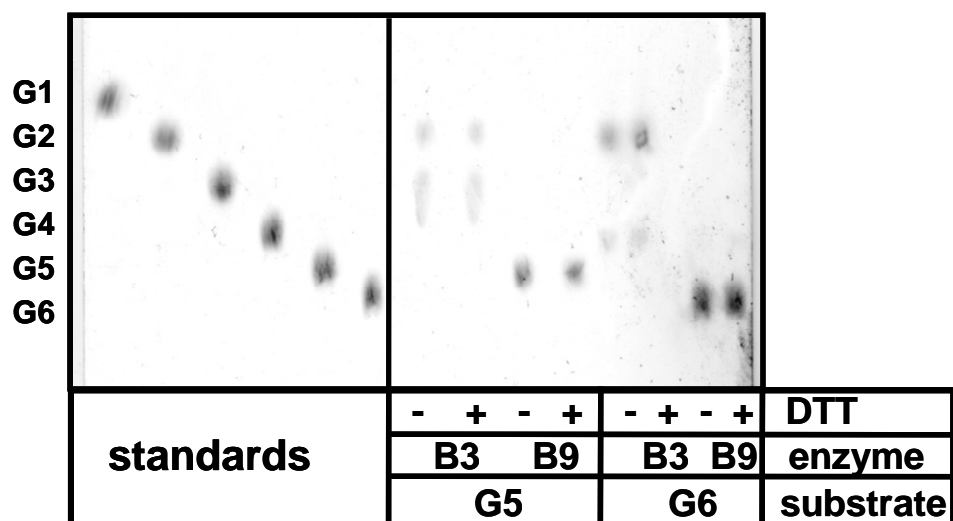


**Figure 19.** Thin Layer Chromatography of oligosaccharide products after incubation with BAM3 and BAM9. BAM3 and BAM9 were incubated with maltopentose and maltohexose for 50 min and heat-inactivated. The products were then separated on a TLC plate. G1-G6 represent the number of glucose residues within the oligosaccharide.

## DISCUSSION

$\beta$ -amylases play an important role in starch degradation. There are nine  $\beta$ -amylase genes found in *Arabidopsis thaliana*. Of the nine BAM proteins, BAM9 has received little attention and its function is unknown. Our first approach was to study the BAM protein sequences using phylogenetic analysis (Figure 4). The Arabidopsis BAM proteins were compared to the rice, grape, and poplar BAM proteins based on amino acid sequence alignments because the genomes of these three species have been sequenced. This resulted in subfamilies similar to those determined by Fulton et al. (2008): BAM1 and -3 in subfamily II, BAM8, -2, and -7 in subfamily IV, BAM5 and -6 in subfamily I, BAM9 and -4 in subfamily III with the non-Arabidopsis BAMX orthologs. Some of the families in our phylogenetic analysis can then be broken into groups including the BAM1, -3 family and the BAM4, -9, -X family. These families can be broken down such that each BAM ortholog creates its own group. All of these BAM proteins, except BAM4, have been found in monocots and eudicots (Figure 4). This could suggest that these individual BAM proteins (BAM1, -3, -9 and, -X) have been important in the evolution of all plants. BAM2, -7, -8, -5, and -6 were not found in separate clades before the monocot/eudicot separation and could have arisen from gene duplication. Grape orthologs were found in every BAM group but this is not the case for poplar and rice. Rice orthologs of Arabidopsis BAM2 and -8 are missing and poplar orthologs of BAM4 and -6 are missing.

These subfamily groupings appear to be consistent with N-terminal localization signals except in the case of BAM5 and -6 and BAM2. BAM5 and -6 are found in different compartments of the cell but both are active (Monroe and Priess, 1990; Zeeman,

personal communication, and Monroe, unpublished). BAM2 is grouped in a subfamily with BAM7 and -8 but BAM2 is missing the N-terminal extension which contains a DNA binding domain. This led Fulton et al. (2008) to suggest the structural change of BAM2 as the reason for BAM2's apparent non-functionality. However, the *bam2,3* double mutant shows an increased levels of starch in younger leaves, suggesting that BAM2 functions in young plants (Monroe unpublished).

An interesting aspect of this phylogenetic tree is that the BAM9 orthologs exist in every species studied and are not grouped with any other  $\beta$ -amylase ortholog. This could imply that BAM9 has an important function that is unique from the other  $\beta$ -amylases.

The expression of *BAM9* was noted as different from other BAMs by Chandler et al. (2001) and Smith et al. (2004). *BAM9* mRNA levels indicated that the gene had a peak of expression at the end of the night. This suggests that the protein may only be present when starch is accumulating during the day, which is opposite of the expression pattern that one would expect from a protein involved in starch degradation (Fulton et al., 2008). Microarray experiments found on the Diurnal website (Oregon State University, <http://diurnal.cgrb.oregonstate.edu/>) are consistent with the results of Chandler et al. (2001) and Smith et al. (2004), showing a diurnal expression pattern for *BAM9* with a peak of expression at the end of the night for all of the different light conditions found on the Diurnal website (Figure 3) except one, suggesting possible circadian regulation. Only when *Arabidopsis* is grown under no-light conditions is the diurnal pattern of *BAM9* disrupted. Under these conditions *BAM9* has a constant low expression (Diurnal website). The expression of *BAM9* also seems to be affected by starvation (Osuna et al., 2007). When *Arabidopsis* was grown under low light conditions and depleted of sucrose, the

level of *BAM9* mRNA increased (Osuna et al., 2007). In one sense, starvation occurs every night when a plant has used up all of the starch that was synthesized during the day. This could be part of the reason the *BAM9* mRNA has such a regular diurnal pattern.

Iodine staining experiments were performed with WT, *bam3*, *bam9* and *bam3,9* knockout mutants that were harvested at the end of the night. The WT leaves had the expected result of undetectable amounts of starch in the leaves, and *bam3* mutants had accumulated starch. One would expect this result because BAM3 is known to be catalytically active with starch in the chloroplasts and should show a starch accumulation phenotype in the leaves when knocked out. This was consistent with the Fulton et al. (2008) study. The *bam9* mutant did not appear to accumulate very much starch from the iodine staining experiment but the *bam3,9* mutant accumulated more starch than the *bam3* mutant.

Starch quantification experiments confirmed these observations (Figure 9). The *bam3* and *bam9* mutants both accumulated more starch than the WT, suggesting that BAM9 does have a function in starch metabolism even though the *bam3* mutant accumulated twice as much starch as *bam9* by the end of the night. The most significant results of this experiment were from the *bam3,9* mutant, which accumulated more than the sum of the two single mutants. This suggests that BAM3 and BAM9 may work together in starch metabolism.

There has been other evidence that the proteins in the  $\beta$ -amylase family work together or even depend on one another to function properly. A study on Arabidopsis BAMs 1-4 shows the levels of starch in single, double, triple and quadruple BAM gene knockouts (Fulton et al., 2008). Two examples that show  $\beta$ -amylase genes depending on

one another are the *bam1,3* and *bam3,4* knockouts. These knockouts were concluded to cause a more severe phenotype than the single knockouts (Fulton et al., 2008). As well, *bam1* did not cause as much of an effect in starch breakdown as *bam3*, just like our results with the *bam3*, *bam9*, and *bam3,9* mutants. Therefore, if the double knockouts with *bam3* cause more severe phenotypes, starch metabolism may work more efficiently when the Arabidopsis BAMs are able to work together.

Crude extract activity assays were conducted to test whether the starch accumulation phenotypes were a result of decreased amylase activity in the mutant plants. The *bam3* mutant had less activity than WT in most experiments (Figures 11 and 12), which was expected because BAM3 is believed to contribute the most amylase activity in the chloroplasts (Fulton et al., 2008). The *bam9* mutant was expected to have the same as or less activity than WT because there was only a small starch accumulation phenotype. However, in the majority of the experiments this mutant had equal to or more activity than WT (Figures 11 and 12). The *bam3,9* mutants were expected to have less activity than the WT based on the starch quantification experiments (Figure 10) and in the majority of the experiments these mutants had less than or equal activity to the WT (Figures 11 and 12). The starch accumulation phenotypes could be due to the fact that the mutants are unable to degrade as much starch every day as the WT (Figure 11). These results imply that BAM9 could be down regulating the activity of BAM3 because when both BAM9 and BAM3 were not present the activity decreased, just as when only BAM3 was knocked out. But when only BAM9 was not present the activity increased and this activity could potentially be attributed to BAM3. Therefore, we hypothesize that BAM9 may down regulate BAM3 in the WT.

We suspect that the variability of activity observed in some experiments is due to BAM5. BAM5 is located in the cytosol (Lin et al., 1988; Monroe and Preiss., 1990; Wang et al., 1995) and our BAM5- GFP experiments have confirmed this (Marafino and Monroe, unpublished). BAM5 has sometimes been found to contribute most of the amylase activity in Arabidopsis leaves (Lin et al., 1988; Laby et al., 2001). Doyle et al. (2007) discovered that its activity increases as leaves get older. The majority of the leaves harvested were between the ages of 4 and 7 ½ weeks old. The younger plants (Figure 11) did show less overall activity than the older plants (Figure 12).

Because there may be a down regulation of BAM3 by BAM9 we studied the microarray data for both the *BAM9* and *BAM3* genes. The expression data showed that as *BAM9* expression was at its peak, *BAM3* expression began to decline. This led us to the hypothesis that BAM9 might down regulate the transcription of *BAM3*. We therefore tested for *BAM3* RNA levels in the *bam9* mutant compared to the WT. If BAM9 down regulated *BAM3* transcription, the level of *BAM3* mRNA in the *bam9* mutant should have been higher than the *BAM3* mRNA in the WT, but no difference was found (Figures 13 and 14). So, the BAM9 protein is not likely to be affecting the transcription of the *BAM3* gene.

In order to further characterize the function of BAM9, *in vitro* studies using the BAM9 purified protein were performed. Using the sequence and structural analysis we were able to suggest possible functions. We first compared the BAM9 amino acid sequence to the active BAM proteins and discovered that BAM9 has a number of differences in the active site. First, the BAM9 binding pocket of the amino acid sequence is missing five conserved residues (Figure 6). Near the active site there is an outer

flexible loop was found in the soybean active BAM (Totsuka and Fukazawa, 1996), which aids in holding starch and releasing maltose during starch degradation (Kang et al., 2004). The missing five residues are the part of the active site that makes up the outer flexible loop (Fulton et al. 2008). BAM9 was predicted to have a different type of activity than other  $\beta$ -amylase genes because there is an absence of the flexible loop (Chandler et al., 2001). Secondly, the conserved residues of the active site in the active BAMs are different from those in BAM9 but are mostly conserved among the BAM9 orthologs (Figure 5). The residues which bind to the first four glucosyl residues of starch in the active BAMs (Mikami et al. 1994) are only conserved in the BAM9 orthologs under the first and second glucose (G1 and G2) binding sites (Figure 5) and we therefore predicted that BAM9 might possibly bind to maltose. However, the third and fourth glucose binding site residues in the Arabidopsis BAM9 are different from the active BAMs but are mostly conserved within the BAM9 orthologs. This could indicate that BAM9 is unable to bind to starch. Though starch hydrolysis by BAM9 seems unlikely, the amino acids in the cleavage site of the BAM9 orthologs are conserved, suggesting that BAM9 is catalytically active with another oligosaccharide (Figure 5).

From the sequence analysis two main hypotheses were generated, 1) BAM9 is not catalytically active with starch and 2) BAM9 is catalytically active with a smaller oligosaccharide. Further support of our second hypothesis developed from the fact that *BAM9* has the opposite pattern of expression as that of Disproportionating enzyme (D-enzyme, DPE1) (Figure 3). D-enzyme is a plastidial  $\alpha$ -1, 4-glucanotransferase (Critchley et al., 2001). In the Critchley et al. (2001) suggested that D-enzyme aids in the metabolism of malto-oligosaccharides (MOS), such as maltotriose, in Arabidopsis.

Critchley et al. (2001) stated that D-enzyme is involved in the breakdown of starch by converting MOS molecules into larger polymers which will allow for other starch degrading enzymes such as  $\beta$ -amylases to degrade them further. Because BAM9 and D-enzyme have opposite patterns of expression, we reasoned that BAM9 may help the plant decrease the amount of the smaller glucan polymers, such as maltotriose, at the end of the night when D-enzyme is not being expressed.

To test our first hypothesis we needed to obtain pure BAM9 protein. His-tagged BAM9 was successfully purified, as evidenced by a band on an SDS-PAGE gel at ~50 kD, which is close to the expected weight of the His-tagged BAM9, 48.8 kD (Figure 15) (Fedkenheur and Monroe, unpublished). Our first hypothesis was tested by measuring the catalytic activity of the purified BAM9 with starch as the substrate. BAM9 had no activity compared to BAM3, which showed about 9 U/mg activity (Figure 17) (Fedkenheur and Monroe, unpublished); therefore, we concluded that BAM9 by itself is not catalytically active with starch. Our second hypothesis was tested by using Thin Layer Chromatography (TLC) to analyze the malto-oligosaccharide products after incubation with BAM9 (Fedkenheur and Monroe, unpublished). In these experiments maltotriose, maltopentose, and maltohexose were used as the substrates. When BAM3 or -9 were incubated with these three substrates BAM3 was observed to have catalytic activity with maltohexose and maltopentose, but was unable to hydrolyze maltotriose (Figures 17 and 18). BAM3 hydrolyzed maltohexose to maltose and broke maltopentose into maltose and maltotriose (Figures 17 and 18). BAM9 did not hydrolyze any of the malto-oligosaccharides into smaller oligosaccharides or monosacchararides. It was concluded that BAM9 by itself is not catalytically active with any of these substrates.



This demonstrated that our original hypothesis for BAM9 as a maltotriose hydrolase was incorrect.

After aligning BAM9 orthologs with BAM3 orthologs, twenty-four amino acid residues were found that were conserved within BAM9 orthologs but different in the BAM3 orthologs. Using BAM9, a three dimensional (3D) model was created with the PHYRE program (Kelly and Sternberg, 2009) (Figure 7). This 3D-model shows that some of the 24 conserved residues are located in a cluster on the outside of the molecule. This cluster includes some hydrophobic amino acids such as Phenylalanine, Proline, and Lysine, which suggests that BAM9 may bind to another molecule, mostly likely another protein. The 3D-model also revealed two cysteines in close proximity to one another indicating that BAM9 is possibly red/ox regulated (Figure 7).

Recently, BAM3 and BAM1 were found to be phosphorylated (Lohrig et al., 2009, and Hazlewood et al., 2010). BAM3 is believed to be active at night (Kaplan and Guy, 2005; Fulton et al., 2008) while BAM1 is believed to be active during the day based on the fact that BAM1 is red/ox regulated is active when it is reduced (Sparla et al., 2006). Many chloroplastic proteins are diurnally regulated by light driven reducing conditions. For the *bam9* mutant to have a starch accumulation phenotype and higher amylase activity than WT, BAM9 would have to be involved in the regulation of the active BAMs. We believe that BAM9 could be involved in the signaling that results in BAM3 being turned off during the day through either phosphorylation or dephosphorlation and BAM1 being turned on during the day through the same or a similar pathway. A chloroplast protein kinase that causes a starch accumulation phenotype when knocked out was recently discovered by Baginsky and Gruissem (2009).

This could be the kinase involved in phosphorylating BAM3 and BAM1 and we propose that BAM9 could function upstream from this kinase. Figure 20 shows a working model of how BAM3, BAM9 and BAM1 may interact with this kinase. We believe that BAM9 may activate the kinase which would in turn inactivate BAM3 and activate BAM1 at the beginning of the light phase. The phenotypes that resulted from the *bam3*, *bam9* and *bam3, 9* mutants are explained in Figure 21. When BAM3 is not present and leaves are harvested at the end of the dark phase one would observe less amylase activity and a large starch accumulation phenotype because BAM3 was not present during the dark phase to degrade starch (Figure 21A). In a *bam9* mutant, BAM3 is never deactivated resulting in more activity, and BAM1 is never activated resulting in a small starch accumulation phenotype (Figure 21B). Finally, when both BAM3 and -9 are not present there is less activity because BAM1 has also not been activated, therefore if both active  $\beta$ -amylases are not functional the result is an extra large starch accumulation phenotype (Figure 21C). To test this model, we plan to quantify starch and amylase activity in both the *bam1* and *bam1,9* mutants. We also plan to obtain knockout mutants of the kinase, measure its amylase activity, and generate mutants with the various *bam* alleles.

The specific function of BAM9 is still unknown but there are a few experiments that could help lead us to its function. First, BAM9 could bind to a carbohydrate; this is supported by the conserved active site amino acids within the BAM9 orthologs. To explore this possibility future work will need to include binding assays using the purified protein with substrates like starch and smaller oligosaccharides, and this is being done in the Monroe lab presently. However, BAM9 could bind to another protein via the cluster of conserved hydrophobic amino acids on the outside of the protein. In order to discover

if this is true we are attempting to identify a BAM9 binding partner (BBP) using the His-tagged BAM9 to probe a cDNA expression library. If a BBP is identified, we predict that the binding of BAM9 to a BBP will be maltose and/or red/ox-sensitive, based on sequence alignments and 3-D modeling.

Finding a BBP or a binding substrate may also indicate if our working model is correct. If a BBP or a binding substrate is not found, the effects of the *bam9* mutant on the expression of other genes would be the next step to finding the function of BAM9. In order to achieve this goal microarray experiments could be done comparing the *bam9* mutant to WT.

The cellular location of BAM9 was found in the chloroplasts (Zeeman, personal communication; Monroe, unpublished), but the expression pattern of BAM9 in the plant has not been fully characterized. This would help us determine the function of BAM9 because different tissues of a plant are involved in different processes. To find in what parts of the plant BAM9 is most prominent, the *BAM9* promoter could be fused to a GUS sequence and introduced into Arabidopsis, as was previously done by Francisco et al. (2010) with *BAM3* and *BAM4*. Finally, BAM9 could be over-expressed in the plant, possibly allowing a phenotype to be observed which may be attributed to the over-expression.

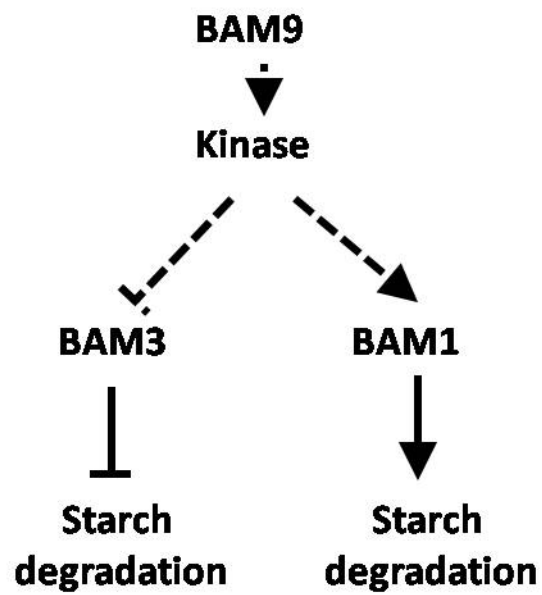


**Figure 20.** A working model for the role of BAM9 in starch metabolism. In this model when BAM9 is present in the cell it functions up stream of a chloroplastic kinase. This kinase then deactivates BAM3 and activates BAM1.

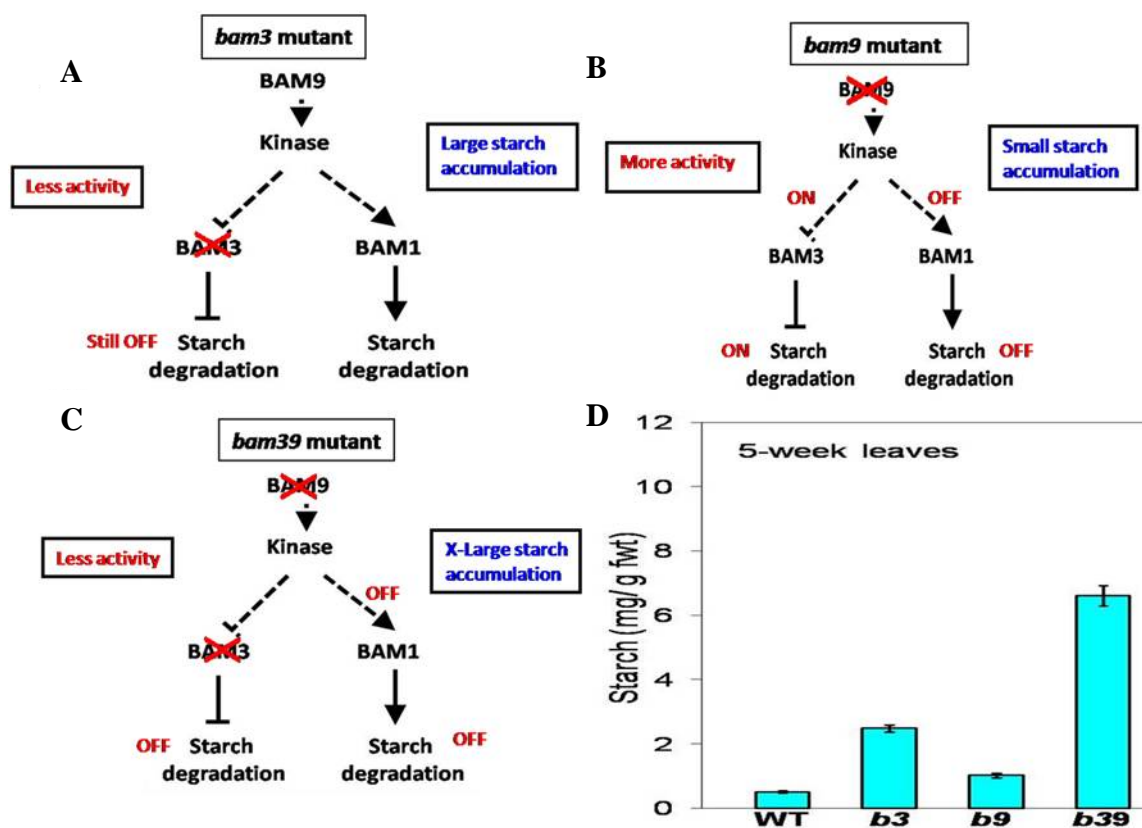


**Figure 21.** The effect of different knockout mutants on the working model of BAM9 function. Each of these conditions depict the effect of leaves harvested at the end of the dark phase, (A) *bam3* mutant plant, (B) *bam9* mutant, and (C) *bam3,9* mutant. D shows the starch accumulation results of each genotype at the end of the night (data from Figure 10).

## LITERATURE CITED

- Baunsgaard, L., Lütken, H., Mikkelsen, R., Glaring, M. A., Pham, T.T., and Blennow, A. (2005) A novel isoform of glucan, water dikinase phosphorylates pre-phosphorylated  $\alpha$ -glucans and is involved in starch degradation Arabidopsis. *The Plant Journal*. 41, 595-605.
- Baginsky, S. and Gruissem, W. (2009) The Chloroplast Kinase Network: New Insights from Large-Scale Phosphoproteome Profiling. *Molecular Plant*. 1–13.
- Chandler, J. W., Apel, S., & Melzer, S. (2001). A novel putative  $\beta$ -amylase gene and AT $\beta$ -amy from *Arabidopsis thaliana* are circadian regulated. *Plant Science (Limerick)* 161, 1019-1024.
- Chang, Y-Y., Liu, H-C., Hsu, F-C., and Ko, S-S. (2006) Arabidopsis Hsa32, a Novel Heat Shock Protein, Is Essential for Acquired Thermotolerance during Long Recovery after Acclimation. *Plant Physiology*. 140, 1297–1305.
- Critchley, J. H., Zeeman, S. C., Takaha, T., Smith, A. M., & Smith, S. M. (2001). A critical role for disproportionating enzyme in starch breakdown is revealed by a knock-out mutation in *Arabidopsis*. *The Plant Journal* 26, 89-100.
- Delatte, T., Umhang, M., Trevisan, M., Eicke, S., Thorneycroft, D., Smith, S. M., Zeeman, S. C. (2006) Evidence for distinct mechanisms of starch granule breakdown in plants. *The Journal of Biological Chemistry*. 281, 12050-12059.
- Edner, C., Li, J., Albrecht, T., Mahlow, S., Hejazi, M., Hussain, H., Kaplan, F., Guy, C., Smith, S. M., Steup, M., and Ritte, G. (2007) Glucan, water dikinase activity stimulates breakdown of starch granules by plastidial beta-amylases. *Plant Physiology*. 145, 17-28.
- Fulton, D. C., Stettler, M., & Mettler, T. et al. (2008). Beta-AMYLASE4, a noncatalytic protein required for starch breakdown, acts upstream of three active beta-amylases in *Arabidopsis* chloroplasts. *The Plant Cell* 20, 1040-1058.
- Fulton DC, Stettler M, Mettler T, Vaughan CK, Li J, Francisco P, Gil M, Reinhold H, Eicke S, Messerli G, Dorken G, Halliday K, Smith AM, Smith SM, and Zeeman SC.(2008) Beta-AMYLASE4, a noncatalytic protein required for starch breakdown, acts upstream of three active beta-amylases in *Arabidopsis* chloroplasts. *Plant Cell*. 20, 1040-58.
- Francisco P, Li, J., and Smith, S. (2010) The gene encoding the catalytically inactive  $\beta$ -amylase BAM4 involved in starch breakdown in *Arabidopsis* leaves is expressed preferentially in vascular tissues in source and sink organs. *Journal of Plant Physiology*. 1-6.

- Heazlewood, J. L., Durek, P., Hummel, J., Selbig, J., Weckwerth, W., Walther, D., Schulze, W. X. (2008) PhosPhAt: a database of phosphorylation sites in *Arabidopsis thaliana* and a plantspecific phosphorylation site predictor. *Nucleic Acids Research*. 36, 1015-1021.
- Kang, Y. N., Adachi, M., Utsumi, S. and Mikami, B. (2004). The roles of Glu186 and Glu380 in the catalytic reaction of soybean  $\beta$ -amylase. *Journal of Molecular Biology* 339, 1129-1140.
- Kaplan, F., and Guy, C. L. (2005). RNA interference of *Arabidopsis* beta-amylase8 prevents maltose accumulation upon cold shock and increases sensitivity of PSII photochemical efficiency to freezing stress. *Plant Journal* 44, 730-743.
- Kaplan F., and Guy, C. L. (2004).  $\beta$ -Amylase induction and the protective role of maltose during temperature shock. *Plant Journal* 135, 1674-1684.
- Kelley L. A. and Sternberg M. J. E. (2009) Protein structure prediction on the web: a case study using the Phyre server. *Nature Protocols*. 4, 363-371.
- Kötting, O., Pusch, K., Tiessen, A., Geigenberger, P., Steup, M., and Ritte, G., (2005) Identification of a novel enzyme required for starch metabolism in *Arabidopsis* leaves. The phosphoglucan, water dikinase. *Plant Physiology*. 137, 242-252.
- Kötting, O., Santelia, D., Edner, C., Eicke, S., Marthaler, T., Gentry, M. S., Comparot-Moss, S., Chen, J., Smith, S. M., Steup, M., Ritte, G., and Zeeman, S.C. (2009) Starch-excess 4 is a laforin-like phosphoglucan phosphatase required for starch degradation in *Arabidopsis thaliana*. *Plant Cell*. 21-334-346.
- Laby, R. J., Kim, D., and Gibson, S. I. (2001) The ram1 mutant of *Arabidopsis* exhibits severely decreased  $\beta$ -amylase activity. *Plant Physiology*. 127, 1798–1807.
- Laederach A, Dowd MK, Coutinho PM, and Reilly PJ. (1999) Automated docking of maltose, 2-deoxymaltose, and maltotetraose into the soybean beta-amylase active site. *Proteins* 37, 166-75.
- Lao N. T., Schoneveld, O., Mould, R. M., Hibberd, J. M., Gray, J. C., and Kavanagh, T. A. (1999). An *Arabidopsis* gene encoding a chloroplast-targeted beta-amylase. *The Plant Journal : For Cell and Molecular Biology* 20, 519-527.
- Laurila, K and Bohlen, M. (2007) Biopolymers as protection during transport of construction materials. *Hogskolaniboras, Instituionen Ingenjorshogskolan*. 1-62.
- Lin T-P., Spilatro S. R., and Preiss J. (1988) Subcellular localization and characterization of amylases in *Arabidopsis* leaf. *Plant Physiology*. 86, 251–259.

- Lloyd J. J. R., Kossmann J., and Ritte G. (2005). Leaf starch degradation comes out of the shadows. *Trends in Plant Science* 10, 120-127.
- Lohrig, K., Muller, B., Davydova, J., Leister, D., and Wolters, D A. (2009) Phosphorylation site mapping of soluble proteins: bioinformatical filtering reveals potential plastidic phosphoproteins in *Arabidopsis thaliana*. *Planta*. 229, 1123-1134.
- Mikami B., Hehre E. J., Sato M., Katsube Y., Hirose M., Morita Y., and Sacchettini J. C. (1993) The 2.0-Å Resolution of Soybean  $\beta$ -amylase Complexed with  $\alpha$ -Cyclodextrin. *Biochemistry* 32, 6838-6845.
- Mikolos, D. A. and Freyer, G. A. (1990) DNA Science: A First Course in Recombinant DNA Technology. Cold Spring Harbor Laboratory Press.
- Mockler T.C., Michael T.P., Priest, H.D., Shen R., Sullivan C.M., Givan S.A., McEntee C., Kay S.A., and Chory, J. (2007) THE DIURNAL PROJECT: Diurnal and Circadian Expression Profiling, Model-Based Pattern Matching and Promoter Analysis. *Cold Spring Harb Symp Quant Biol.* 72:353-363.
- Michael T.P., Mockler T.C., Breton G., McEntee C., Byer A., Trout J.D., Hazen S.P., Shen R., Priest H.D., Sullivan C.M., Givan S.A., Yanovsky M., Hong F., Kay S.A., and Chory J. (2008) Network Discovery Pipeline Elucidates Conserved Time of Day Specific cis-Regulatory Modules. *PLoS Genetics*. 4(2):e14.
- Monroe J. D. and Preiss, J. (1990). Purification of a  $\beta$ -Amylase that Accumulates in *Arabidopsis thaliana* Mutants Defective in Starch Metabolism. *Plant Physiology* 94, 1033.
- Monroe, J. D., Salminen, M. D., and Preiss, J. (1991) Nucleotide Sequence of a cDNA Clone Encoding a  $\beta$ -Amylase from *Arabidopsis thaliana*. *Plant Physiology*. 97, 1599-1601.
- Nelson, N. (1944). A Photometric Adaptation of the Somogyi Method For The Determination of Glucose. May Institute for Medical Research of the Jewish Hospital, and the Department of Biological Chemistry, College of Medicine, University of Cincinnati, Cincinnati. 375-380.
- Niittylä, T., Messerli, G., Trevisan, M., Chen, J., Smith, A. M., and Zeeman, S. C. (2004) A previously unknown maltose transporter essential for starch degradation in leaves. *Science*. 303, 87-89.
- Osuna, D., Usadel, B., Morcuende, R., Gibon, Y., Bla, O. E., Ho, M., Gu, M. (2007) Temporal responses of transcripts, enzyme activities and metabolites after adding sucrose to carbon-deprived *Arabidopsis* seedlings. *The Plant Journal*. 49: 463-491.



- Ritte, G., Lorberth, R., and Steup, M. (2000) Reversible binding of the starch-related R1 protein to the surface of transitory starch granules. *The Plant Journal* 21, 387-391.
- Ritte, G., Heydenreich, M., Mahlow, S., Haebel, S., Kottling, O., and Steup, M. (2006) Phosphorylation of C6 and C3-positions of glucosyl residues in starch is catalysed by distinct dikinases. *FEBS Letters*. 580, 4872-4879.
- Scheidig, Andreas A., Frohlich, A. Schulze, S., Lloyd, J. R., and Kossmann, J. (2002). Downregulation of a chloroplast-targeted beta-amylase leads to a starch-excess phenotype in leaves. *The Plant Journal: For Cell and Molecular Biology* 30, 581-591.
- Smith, S. S. M., Fulton, D. C., Chia, T., Thorneycroft, D., Chapple, A., Dunstan, H., Hylton, C. Zeeman, S. C., and Smith, A. M. (2004). Diurnal Changes in the Transcriptome Encoding Enzymes of Starch Metabolism Provide Evidence for Both Transcriptional and Posttranscriptional Regulation of Starch Metabolism in Arabidopsis Leaves. *Plant Physiology* 136, 2687-2699.
- Sparla, F. F., Costa, A., Schiavo, F. L., Pupillo, P., and Trost, P. (2006). Redox Regulation of a Novel Plastid-Targeted beta-Amylase of Arabidopsis. *Plant Physiology* 141, 840-850.
- Stanley, D., Fitzgerald, A. M., Farnden, K. J. F., McRae, E. A. (2002) Characterization of putative amylases from apple (*Malus domestica*) and *Arabidopsis thaliana*. *Biologia* 57, 137-148.
- Totsuka, A., Nong, V. H., Kadokawa, H., Kim, C-S., Itoh, Y., and Fukazawa, C., (1994) Residues essential for catalytic activity of soybean  $\beta$ -amylase. *European Journal of Biochemistry*. 221, 649-654.
- Totsuka, A. and Fukazawa, C. (1996). Functional analysis of Glu380 and Lew383 of soybean  $\beta$ -amylase a proposed action mechanism. *European Journal of Biochemistry* 240, 655-659.
- Wang, Q., Monroe, J., and Sjolund, R. D. (1995) Identification and Characterization of a Phloem-Specific  $\beta$ -Amylase Plant Physiology. 109, 3, 743-750.
- Weise S.E., Weber, A. P., and Sharkey, T. D. (2004). Maltose is the major form of carbon exported from the chloroplast at night. *Planta* 218, 474-482.
- Yu, T-S., Kofler, H., Hausler, R., E., Hille, D., Flugge, U-I, Zeeman, S. C., Smith, A. M., Kossmann, J., Lloyd, J., Ritte, G., Steup, M., Lue, W-L., Chen, J., and Weber, A., (2001) SEX1 is a general regulator of starch degradation in plants and not the chloroplasts hexose transporter. *Plant Cell* 13, 1907-1918.

- Yu, T-S., Zeeman, S., C., Thorneycroft, D., Fultn, D. C., Dunstan, H., Lue, W-L., Hegemann, B., Tung, S-Y., Umemoto, T., Chapple, A., Tasi, D. D., Wang, S. M., Smith A. M., Chen, J., and Smith, S. M. (2005)  $\alpha$ -Amylase is not required for break down of transitory starch in *Arabidopsis* leaves. *Journal of Biological Chemistry*. 280, 9773-9779.
- Zeeman, S. C., Northrop, F., Smith, A. M., ap Rees, T. (1998) A starch-accumulating mutant of *Arabidopsis thaliana* deficient in a chloroplastic starch-hydrolyzing enzyme. *The Plant Journal* 15, 357-365.
- Zeeman S.C., Tiessen, A., Pilling, E., Kato, K.L., Donald, A. A., and Smith, A. M. (2002). Starch Synthesis in *Arabidopsis*. Granule Synthesis, Composition, and Structure. *Plant Physiology*, 129, 516-529.